Naval Research Laboratory

Washington, DC 20375-5320

NRL/FR/6930--16-10,290

Development of Sorbents for Extraction and Stabilization of Nucleic Acids

BRANDY J. WHITE

Laboratory for Molecular Interfaces
Center for Bio/Molecular Science and Engineering

BRIAN J. MELDE

Laboratory for Molecular Interfaces
Center for Bio/Molecular Science and Engineering

BAOCHUAN LIN

Laboratory for Biomaterials and Systems
Center for Bio/Molecular Science and Engineering

September 13, 2016

REPORT DOCUMENTATION PAGE

Form Approved
OMB No. 0704-0188

1. REPORT DATE *(DD-MM-YYYY)*	**2. REPORT TYPE**	**3. DATES COVERED** *(From - To)*
13-09-2016	Formal Report	1 October 2011 to 30 September 2015

4. TITLE AND SUBTITLE

Development of Sorbents for Extraction and Stabilization of Nucleic Acids

5a. CONTRACT NUMBER

5b. GRANT NUMBER

5c. PROGRAM ELEMENT NUMBER

6. AUTHOR(S)

Brandy J. White, Brian J. Melde, and Baochuan Lin

5d. PROJECT NUMBER

5e. TASK NUMBER

5f. WORK UNIT NUMBER
69-6595

7. PERFORMING ORGANIZATION NAME(S) AND ADDRESS(ES)

Naval Research Laboratory
4555 Overlook Avenue, SW
Washington, DC 20375-5320

8. PERFORMING ORGANIZATION REPORT NUMBER

NRL/FR/6930--16-10,290

9. SPONSORING / MONITORING AGENCY NAME(S) AND ADDRESS(ES)

Naval Research Laboratory
4555 Overlook Avenue, SW
Washington, DC 20375-5320

10. SPONSOR / MONITOR'S ACRONYM(S)

NRL

11. SPONSOR / MONITOR'S REPORT NUMBER(S)

12. DISTRIBUTION / AVAILABILITY STATEMENT

Approved for public release; distribution is unlimited.

13. SUPPLEMENTARY NOTES

14. ABSTRACT

This effort focused on development of a combined storage and delivery system intended to offer much-needed stability to biomolecules, especially DNA and RNA. The goal was to provide stabilization methods for reagents and targets in order to allow for a wider range of applications through utilization of organized porous materials as scaffolds for their encapsulation. This report details the synthesis of solid support materials, selection of stabilization components, and development of methods for their application. Design considerations focused on control of interactions with the nucleic acids that result in degradation. Over the course of the effort, the potential for adsorption of RNA, DNA, and ssDNA onto porous organosilicate sorbents with and without additional stabilizing reagents was demonstrated. Improved binding capacities were achieved with sorbents using chemical functionalities rather than proteins and sugars. These sorbents were found to provide similar improvements in stability to the traditional stabilization compounds. The materials were further shown to provide capture and subsequent stabilization of targets from a complex solution.

15. SUBJECT TERMS

Organosilicate	RNA	Capacity	Transport
DNA	Stability	Field sampling	

16. SECURITY CLASSIFICATION OF:			**17. LIMITATION OF ABSTRACT**	**18. NUMBER OF PAGES**	**19a. NAME OF RESPONSIBLE PERSON**
					Brandy J. White
a. REPORT	**b. ABSTRACT**	**c. THIS PAGE**	Unclassified Unlimited	40	**19b. TELEPHONE NUMBER** *(include area code)*
Unclassified Unlimited	Unclassified Unlimited	Unclassified Unlimited			202-404-6100

Standard Form 298 (Rev. 8-98)
Prescribed by ANSI Std. Z39.18

This page
intentionally
left blank

CONTENTS

EXECUTIVE SUMMARY E-1

INTRODUCTION 1

- Stabilizing Nucleic Acids 2
- Porous Materials 3

SYNTHESIS AND CHARACTERIZATION OF SORBENT MATERIALS 5

- Synthetic Protocols 5
- Characterization Methods 8
- Morphological Characteristics 8

TARGET BINDING FROM AQUEOUS SOLUTION 13

- RNA, DNA, and ssDNA Preparation 13
- Nucleic Acid Adsorption and Elution Protocols 13
- Real-Time Reverse Transcription PCR and Real-Time PCR 14
- Target Adsorption 14

ELUTION OF BOUND TARGETS 17

STABILITY 22

CAPTURE FROM COMPLEX SOLUTIONS 24

- Bacterial Lysis 24
- Target Adsorption 25

CONCLUSIONS 26

ACKNOWLEDGMENTS 26

REFERENCES 26

This page
intentionally
left blank

EXECUTIVE SUMMARY

October 2012, the Center for Bio/Molecular Science and Engineering at the U.S. Naval Research Laboratory (NRL) began an effort to develop a combined storage and delivery system to offer much-needed stability to biomolecules, especially DNA and RNA. The goal was to provide a way to stabilize reagents and targets by using organized porous materials as scaffolds for their encapsulation. This report details the synthesis of solid support materials, selection of stabilization components to incorporate within the scaffolds, and optimal methodologies for using the systems to capture, stabilize, and recover nucleic acids.

Sorbent design considerations focused on control of interactions with the nucleic acids that result in degradation. Adsorption or encapsulation can restrict some of these interactions, such as access of enzymes and microorganisms, and the mobility of the nucleic acids. Other useful sorbent characteristics include components that alter solvent interactions, provide reducing sites and chelating groups, and inhibit nuclease activity. The early focus of the NRL study was on incorporating common sugars and bovine serum albumin (BSA) as stabilizing agents. Later work evaluated incorporating chemical functionalities into the sorbents to address other aspects of nucleic acid degradation. Several sorbent materials were developed and the following properties were evaluated: the capacity of the sorbent to bind RNA, DNA, and single stranded DNA (ssDNA); the ability to recover by elution the bound material from the sorbent; and the impact of the sorbent on long-term sample viability.

We have demonstrated RNA, DNA, and ssDNA adsorption onto porous organosilicate sorbents with and without additional stabilizing reagents. The NRL-developed sorbents provided enhanced stability for extended periods, allowing the adsorbed targets to be eluted using simple buffers and employed directly for downstream molecular diagnostic assays. Improved binding capacities were achieved with sorbents using chemical functionalities. These sorbents were found to provide similar improvements in stability to traditional stabilization compounds (sugars and BSA). The materials were further shown to provide capture and subsequent stabilization of targets from a complex solution.

This page
intentionally
left blank

DEVELOPMENT OF SORBENTS FOR EXTRACTION AND STABILIZATION OF NUCLEIC ACIDS

INTRODUCTION

In October 2012, the Center for Bio/Molecular Science and Engineering at the U.S. Naval Research Laboratory (NRL) began research to develop a combined storage and delivery system to provide much-needed stability to biomolecules, especially DNA and RNA, during storage and shipment. The goal was to provide stabilization methods for reagents and nucleic acid (NA) targets by using organized porous materials as scaffolds for their encapsulation.

Nucleic acid–based technologies are used in the detection and identification of threats, collection of forensic information on the origin or progression of a threat, biosurveillance, and other applications significant to the Department of Defense. Technologies based on molecular diagnostics offer the potential to ensure safe food and water supplies and to maintain the health and readiness of deployed troops. Identification of molecular signatures (genomic information) for pathogens can increase situational awareness.

Unfortunately, application of NA-based technologies is limited by reagent instability and short shelf life, special storage requirements for the reagents and samples (usually refrigeration, an energy-intensive activity that places great logistical demands on deployed units), and incompatibility of reagents and samples with solvent/surfactant systems. Field applications would significantly benefit from stabilization of the reagents, for use in basic on-site analyses, and of the samples collected, to preserve them for detailed analysis at distant laboratories. Elimination of the need for special storage conditions would vastly extend the application of genetics-based detection both in the field and at laboratories, offer enhanced protective capabilities to fielded troops, and reduce the logistical demands of techniques currently in use. In addition, stabilizing technologies can provide new sampling methodologies that can enhance the capacity for obtaining environmental data.

In the absence of stabilizing compounds, nucleic acids have a short functional lifetime (minutes to hours). Stabilizing agents extend the functional lifetime of the nucleic acids, but these agents often interfere with intended downstream applications such as polymerase chain reaction (PCR) or reverse transcription. A system is needed that provides stability to NAs without these competitive effects. In addition, the system should have a controllable delivery mechanism that allows for the dissociation of NAs from the scaffold at a desired time. The mechanism could involve a particular set of chemical conditions, for example, or exposure to low-energy UV excitation. Entrapment of biomolecules within a confined space to overcome chemical and thermal instability is an area of active research interest. The commonly used methods provide a certain degree of success; however, the low availability of surface area and the harsh conditions needed to immobilize biomolecules counterbalance the stability provided. The research described here seeks to utilize organized porous materials for the stabilization of NAs to overcome the shortfalls of other approaches.

Manuscript approved August 15, 2016.

Stabilizing Nucleic Acids

Advancements in molecular diagnostics related to a wide range of fields, including medical, biological, environmental, forensics, and food safety, drive the need for preservation of nucleic acid integrity during sample collection, transportation, processing, and storage [1]. RNA tends to be more labile than DNA and can be hydrolyzed readily when exposed to high pH, metal cations, high temperatures, or contaminating RNA ribonucleases (RNases). RNases, the primary contributor to RNA degradation, are known to be present endogenously in cells, tissues, body oils, and bacteria and fungi in airborne dust particles [2]. A number of commercial products are available for preserving RNA during sample collection: RNAlater Tissue Collection: RNA Stabilization Solution (Life Technologies, Carlsbad, CA), RNAlater RNA Stabilization Reagent (Qiagen, Valencia, CA), PAXgene tubes (PreAnalytix, Valencia, CA), and RNAstable (Biomatrica, San Diego, CA). Alternatively, RNA can be protected within a physical barrier by employing materials similar to those used in DNA encapsulation: liposomes, micelles, or polymers [3–6]. RNA encapsulation methods have been used mainly as delivery systems for small interfering RNA (siRNA) [3,4,6–8]. Encapsulation of RNA within these types of tunable, semipermeable structures has not been fully explored for stabilization and storage purposes.

The most common method for maintaining nucleic acid integrity, in general, is freezing at low temperature (−20 °C or −80 °C) [9]. However, this approach is not practical for routine specimen processing, storage, or shipping related to austere field conditions. Furthermore, the costs associated with maintaining large sets of samples under the necessary conditions over long periods of time can be prohibitive [10–12]. To address these disadvantages, several technologies have been developed for stabilization and storage of nucleic acids at room temperature. These technologies are based primarily on three principles. The first is anhydrobiosis, the dehydration process used by some organisms to survive extreme conditions [13,14]. These methods include spray drying, spray-freeze-drying, air drying, and lyophilization with or without additives (such as trehalose) and are commonly used for DNA preservation [15–19]. One study indicated that anhydrobiosis could be applied to RNA preservation [20]. While in the dry state, the matrix components form a thermo-stable barrier around the DNA, protecting the sample from damage and degradation. The DNA can be recovered by rehydration, as the matrix will completely dissolve [11,21,22]. The second approach to stabilization is to use chemicals or proteins to bind nucleic acids, changing their characteristics and interactions to provide stability. Several chemicals and compounds have been reported to preserve nucleic acids at room temperature for weeks to months. DNA-binding protein from starved cells (Dps) and poly(A) binding protein (Pab1p) were reported to stabilize DNA and mRNA, respectively [12,23–38]. Commercial products such as RNAlater and Trizol (Life Technologies) are based on this approach and have been documented to stabilize nucleic acids at room temperature for long periods of time [11,27,30,39–41]. Physically protecting nucleic acids from the environment, through encapsulation or adsorption onto a solid support, is the third of the stabilization principles and has emerged for the delivery of gene therapeutics. A range of materials, including liposomes, metal particles, mesoporous silica nanoparticles (MSNs), polymers, potato starch, silk fibron, and surfactants, have been developed with these applications in mind [3,42–49].

Porous Materials

The scaffolds considered here are comprised of condensed silsesquioxane precursors that produce mesoporous materials, including MSNs, mesoporous silica nanoparticles, and PMOs, periodic mesoporous organosilicates.

MSNs are synthesized using tetraethyl orthosilicate (TEOS) to form the structure (Fig. 1) [53]. Coordination of the TEOS precursor with an ionic surfactant results in the desired organizational characteristics. The resulting materials have pore walls with alternating silicon and oxygen atoms. These structures can be modified following synthesis to incorporate stabilizing compounds. MSNs offer high surface areas and ordered or semi-ordered pore structures. Reaction conditions can be chosen to yield relatively monodisperse particle sizes (50–200 nm). Small particle sizes allow for capping of mesopores or other modifications that may prevent undesired release of encapsulated cargo. The nanoparticle morphology also offers advantages in adsorption rates and saturation loading levels [50–53]. Previous studies have applied MSN materials to biosensing and controlled delivery [54–57]. Materials of this type have also been shown to provide stability to proteins through adsorption interactions, as well as through covalent immobilization [58–61].

PMOs are organic–inorganic materials with ordered pore networks and large internal surface areas (up to 1000 m^2/g). These materials are synthesized using different approaches to obtain varied final products. Typically, sorbents are synthesized using high concentrations of nonionic surfactants (Fig. 2) [62–64] in which liquid crystal–like phases are formed prior to addition of precursor compounds. This approach provides the potential for use of a broad range of compounds in forming the pore walls and offers control over the final morphological characteristics of the materials. The resulting materials have narrow pore size distributions with few blocked pores or obstructions, facilitating molecular diffusion throughout the pore networks. The alternating siloxane and organic moieties give PMOs properties associated with both organic and inorganic materials [65]. The siloxane groups provide the structural rigidity required to employ surfactant templating methods, which provide precise control when engineering porosity. In addition to structural rigidity, the silica component of the PMOs provides a degree of hydrophilic character useful for applications in aqueous systems. This allows for entrapment of biomolecules under neutral mild conditions. Incorporation of organic functional groups within materials provides target interactions that are typically associated with organic polymers. These unique characteristics make these scaffold materials ideal for entrapment of biomolecules. The versatility of the materials also makes it possible to covalently link stabilizing agents within the pores, potentially extending the utility of stabilization compounds identified by previous studies by avoiding the problem of downstream contamination.

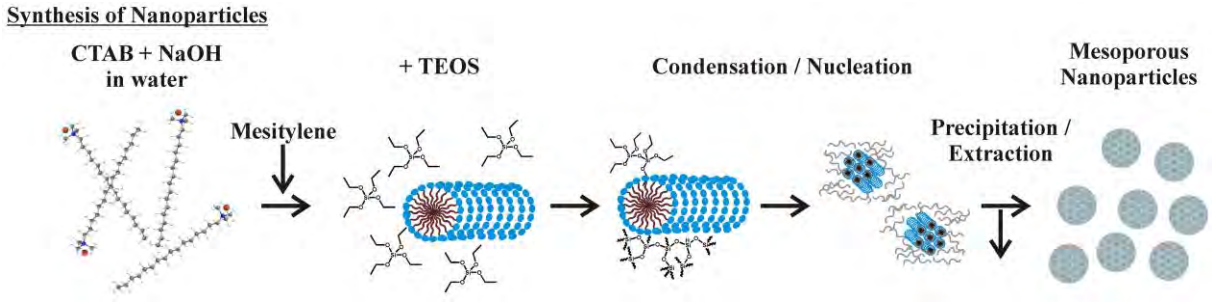

Fig. 1 — Synthesis of mesoporous silicate nanoparticles (MSNs) [53,66]. Compounds are defined in the discussion.

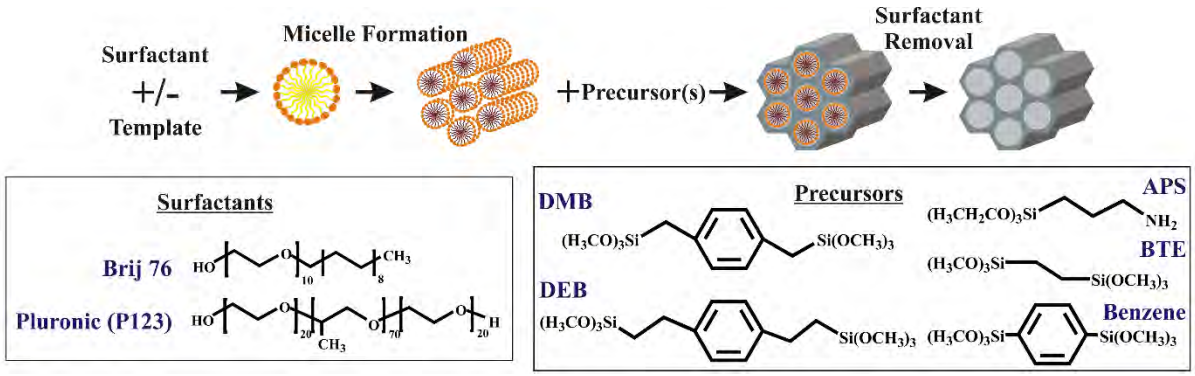

Fig. 2 — Synthesis of organosilicate sorbents is accomplished by condensing precursors around surfactant micelles under appropriate conditions [67,68]. Compounds are defined in the discussion.

SYNTHESIS AND CHARACTERIZATION OF SORBENT MATERIALS

A number of standard processes were used to synthesize the various sorbents evaluated. This section describes synthesis of the sorbents and presents results of morphological characterization. Table 1 lists the materials synthesized.

Table 1 — Sorbent Materials and Characteristics

Material	Description	Surface Area (m^2/g)	Pore Volume (cm^3/g)	Pore Diameter (Å)
NS	Bare silicate nanoparticle sorbent; no organic groups	730	0.75	50
NS-T	NS sorbent modified with trehalose	320	0.31	50
NS-G	NS sorbent modified with glucosamine	320	0.31	50
NS-B	NS sorbent modified with BSA	166	0.26	50
N5	Primary amine groups on BTE sorbent	1002	1.19	77
P5	Phenyl groups on DEB sorbent	470	0.46	50
P10	Phenyl groups on DEB sorbent	440	0.43	43
MM5	DEB sorbent	606	0.51	44
CuEDA	Coordinated copper on BTE sorbent	716	0.87	64
ZnEDA	Coordinated zinc on BTE sorbent	275	0.70	223
HX2M2B	Alkylammonium groups on ordered pore structure (TMOS)	169	0.26	63
CF2M2B	Alkylammonium groups on mesostructured cellular foam (TMOS)	143	0.18	93
CF-BT	BSA and trehalose adsorbed on mesostructured cellular foam (TMOS) with alkylammonium groups	236	0.36	111
CF-B*	BSA immobilized on mesostructured cellular foam (TMOS) with alkylammonium groups	--	--	--
CF-T*	Trehalose immobilized on mesostructured cellular foam (TMOS) with alkylammonium groups	--	--	--
CF-2X*	BSA and trehalose immobilized on mesostructured cellular foam (TMOS) with alkylammonium groups	--	--	--
DEN	Amine and C12 terminated dendrimer on BTE sorbent	649	0.75	40
ChTS	Chitosan on TEOS	550	0.82	54
ChMS	Chitosan covalently incorporated into glycidoxy-functionalized sorbent	440	0.55	71

*Morphological data not collected for all CF variants.

Synthetic Protocols

Synthesis of mesoporous silicate nanoparticles was adapted from a published procedure [55]. Briefly, 1.0 g of CTAB (cetyltrimethylammonium bromide, a cationic surfactant) was dissolved at 80 °C in 475 mL water and 7.0 mL 1.0 M NaOH with stirring. The reactor vessel was a polyethylene bottle suspended in a

temperature-controlled water bath. Mesitylene (TMB, 6 mL) was added to the stirring surfactant solution. Tetraethyl orthosilicate (TEOS, 5.0 mL) was added drop-wise, and a white precipitate formed. The mixture was stirred and heated at 80 °C, collected by filtration, and allowed to dry at room temperature. As-synthesized material was refluxed in 160 mL of ethanol with 5 mL of concentrated HCl overnight. MSNs were separated from the acidified ethanol by centrifugation. They were suspended in ethanol, centrifuged, and resuspended three times in water followed by centrifugation each time. Extracted MSNs were dried at 80 °C.

Modification of the silicate structure by stabilizing compounds was accomplished by first providing functional groups on the silicate surface. Materials (1 g) were refluxed with the appropriate precursor (3-aminopropyltrimethoxysilane, APS, or 3-isocyanatopropyltriethoxysilane, ICS; 22 μM) in toluene overnight [69]. Functionalized materials were recovered using vacuum filtration with Whatman #5 filter paper, rinsed with toluene, and dried at 110 °C. For immobilization of sugars, the ICS-functionalized sorbent (1 g) was placed in solution with an excess of the sugar (1 g in 0.25 L). The solution was then mixed for 48 h before the material was recovered by vacuum filtration, thoroughly rinsed with deionized water to remove excess, unbound sugar, and dried at 60 °C for 24 h. For immobilization of bovine serum albumin (BSA), EDC (1-ethyl-3-[3-dimethylaminopropyl]carbodiimide) chemistry was used. APS-functionalized silicate material (1 g) was placed with 1 g BSA in a solution of 5 mM EDC in 100 mM MES buffer (2-(N-morpholino)ethanesulfonic acid; pH 5.5). The solution was incubated with agitation overnight, rinsed thoroughly with water, and dried at 50 °C for 24 h.

Synthesis of the bis(trimethoxysilylethyl)benzene (DEB) and 1,2-bis(trimethoxysilyl)ethane (BTE) based sorbents (MM5, P10, P5, N5, and DEN) was based on a previously described approach [49,70,71] and began with dissolving various quantities (as indicated) of TMB and Pluronic P123 surfactant (1.9 g) in 0.1 M HNO_3 with stirring at 60 °C. The stirring solution was cooled to room temperature and the silane mixture was added drop-wise. The reaction mixture was stirred until homogeneous and transferred to a culture tube which was sealed tightly and heated at 60 °C overnight (~18 h). The tube was unsealed and the white gel was heated at 60 °C for 2 days and then 80 °C for 2 days. P123 was extracted by refluxing the monolith three times in 1M HCl/ethanol for at least 12 h. A powdered product was collected by suction filtration, rinsed with ethanol and water, and dried at 100 °C. For MM5, 0.3 g TMB was used with 6 g 0.1 M HNO_3. The total mol Si used was 7.84 mmol with 50:50 BTE:DEB. For P10 and P5, 0.55 g TMB was used with 7.5 g 0.1 M HNO_3. The silane mixture consisted of 15.7 mmol total Si with either 50:40:10 (P10) or 50:45:5 (P5) BTE:DEB:PTS (phenyltrimethoxysilane).

For N5, the protocol utilized 0.3 g TMB with 9.5 g 0.1 M HNO_3 and the silane mixture was 100% BTE [49]. Following synthesis, amine groups were grafted on to the materials by adding sorbent (1 g) to 200 mL of toluene with 1 g APS [69]. This mixture was refluxed for 24 h after which the grafted product was collected by vacuum filtration, washed with toluene then ethanol, and dried at 110 °C. The DEN sorbent is a variation of this material. Following the amine functionalization protocol, isocyanate groups were incorporated using the ICS precursor [69]. This sorbent (1 g) was then placed in 50 mL MES buffer (100 mM, pH 5.5) with 1.3 g PAMAM dendrimer (10 wt% in methanol) and mixed on a rotisserie mixer overnight at room temperature. The sorbent was collected by vacuum filtration, washed with methanol, and dried at 110 °C.

The alkylammonium-group-bearing sorbents (HX, CF prefixes) were synthesized based on a published approach [70–72]. The HX sorbent was intended to provide a scaffold with hexagonally packed cylindrical pores while the CF sorbent provides a disordered arrangement of spherical pores sometimes described as a mesostructured cellular foam. For synthesis of the HX sorbent, 4.0 g of Pluronic P123 and 0.85 g of TMB were dissolved in 12.0 g of 1.0 M HNO_3 with magnetic stirring and heating at 60 °C. The stirring mixture was allowed to cool to room temperature and 5.15 g of tetramethoxysilane (TMOS) was added drop-wise. The mixture was stirred until homogeneous, transferred to a culture tube, sealed tightly, and heated at

60 °C overnight (≥18 h). The white monolith was dried in the unsealed tube at 60 °C for approximately 5 days before calcination (ambient atmosphere, temperature ramped 1 °C/min to 650 °C and held for 5 h) to remove surfactant. The CF sorbent was synthesized identically, except the TMB quantity used was 3.10 g. Materials were dried at 110 °C prior to grafting with alkylammonium silanes, which was accomplished by adding sorbent (1 g) to 100 mL of toluene followed by addition of 2 mmol of both *N*-trimethoxysilylpropyl-*N*,*N*,*N*-trimethylammonium chloride (TSPMC) and *N*-trimethoxysilylpropyl-*N*,*N*,*N*-tri-n-butylammonium chloride (TSPBC) to produce the HX2M2B and CF2M2B sorbents. This mixture was refluxed for 24 h after which the grafted product was collected by vacuum filtration, washed with toluene then ethanol, and dried at 110 °C. An additional sorbent, CF1, was synthesized identically except that 0.5 mmol each of TSPMC and TSPBC was used.

CF1 was further functionalized, using approaches described above, to produce multifunctional materials. CF-BT was synthesized by incubating CF1 (100 mg) with 50 mg trehalose and 100 mg BSA in water (15 mL) for 3 h. Following incubation with agitation, the materials were centrifuged and rinsed to remove excess sugar and protein, and they were dried at 110 °C. CF-B was synthesized by incubation of CF1 (100 mg) with APS (0.3 mmol) in toluene (10 mL) for 45 min. After rinsing, the APS-modified material was incubated with BSA (100 mg) in a solution of 5 mM EDC in 100 mM MES buffer pH 5.5. CF-T was synthesized by incubation of CF1 (100 mg) with ICS (0.3 mmol) in toluene (10 mL) for 45 min. After rinsing, the ICS-modified material was incubated with trehalose (100 mg) in phosphate buffered saline (PBS). For synthesis of CF-2X, CF1 (100 mg) was incubated with ICS (0.15 mmol) and APS (0.15 mmol) in toluene (10 mL) for 45 min. After rinsing, the APS/ICS-modified material was incubated with trehalose (50 mg) and BSA (50 mg) in a solution of 5 mM EDC in 100 mM MES buffer pH 5.5.

Metal-functionalized sorbents (CuEDA, ZnEDA) utilized N-(-2-aminoethyl)-3-aminopropyltrimethoxysilane (EDA) for chelation. Synthesis used an adapted protocol [73–75] in which BTE (3.2 g) was dissolved in 0.01 M HCl (4 g). P123 (0.65 g) was added to the mixture and allowed to fully dissolve. The metal chelating group, EDA (0.11 g), was then added with either zinc chloride (0.04 g) or copper chloride (0.04 g) and a vacuum was pulled on the solutions for 24 h. The tube was sealed and placed in an oven at 100 °C for 0.5 h followed by 60 °C for 24 h. Sorbents were refluxed twice in acidified ethanol to remove the surfactant and soaked overnight in an ammonium hydroxide solution. After rinsing, metals were reincorporated through refluxing in a 0.1 M solution of either copper chloride or zinc acetate.

Synthesis of chitosan sorbents (ChTS) utilized a reactor consisting of a 1000 mL PTFE jar set in a water bath maintained at 80 °C. CTAB (1.0 g) and 1.0 N NaOH (6.0 mL) were dissolved in 475 mL water with magnetic stirring [53,66]. TMB (6.0 mL) was added, and the solution was stirred for 3 h. Tetraethyl orthosilicate (5 mL) was added, and the mixture was stirred; white precipitate formed quickly. After 2 h, the precipitate was collected on filter paper by gravity filtration. When dry, the material was refluxed in 160 mL of ethanol with 9 mL of hydrochloric acid (37%) for 1 day to extract surfactant. The extracted product was collected by centrifugation, and washed with ethanol followed by water (three times). The sorbent was dried at 110 °C prior to functionalization. To incorporate chitosan, a mixture of 1 g chitosan and 100 mL of 1 vol% acetic acid was prepared and filtered to remove insoluble matter. The sorbent was magnetically stirred in 50 mL of chitosan solution at room temperature for 1 day. The functionalized material (ChTS) was collected by centrifugation and washed with water three times before drying at 70 °C.

For a different approach to development of a chitosan-functionalized sorbent (ChMS), a (3-glycidoxypropyl)trimethoxysilane-functionalized material was synthesized for covalent anchoring of chitosan by adapting a published procedure [76]. Cetyltrimethylammonium chloride reagent (2.67 g; 25% in water) was diluted with 24 g of water in a 60 mL PTFE jar and heated in an oven at 60 °C. In a separate 120 mL PTFE jar, a two-phase mixture was made of 14.3 g triethanolamine with 2.083 g TEOS and 0.48 g (3-glycidoxypropyl)trimethoxysilane; the mixture was heated at 90 °C in an oven for at least 20 min. The two heated mixtures were removed from the ovens and combined immediately; the combined mixture was

stirred at 600 rpm for 3 h at room temperature. Ethanol (50 mL) was added and the precipitate was collected by centrifugation. The solid was washed with ethanol and centrifuged. The precipitate was dried at 60 °C. Cetyltrimethylammonium chloride surfactant was ion-exchanged by dispersing the material in 50 mL NH_4NO_3 /ethanol solution (20 g/L), stirring and heating at 60 °C overnight. The material was collected by centrifugation and washed with ethanol. After drying the material at 80 °C, the ion-exchange process was repeated two more times with fresh NH_4NO_3 solution. The material was washed with ethanol, centrifuged, and washed with water. A second ion-exchange was performed by stirring the material in 50 mL HCl/ethanol solution (5 g/L concentration) at room temperature for 1 day. Material was collected by centrifugation, washed once with ethanol and twice with water. The product was dried first at 60 °C in centrifuge tubes that were lightly capped overnight, then uncapped and dried thoroughly at 80 °C. A 2 wt% chitosan oligosaccharide lactate solution was prepared in 1 wt% acetic acid. The silicate material was stirred in 50 g of chitosan oligosaccharide lactate solution at 60 °C for 1 day. Material was collected by centrifugation, washed four times with water, and dried at 60 °C.

Characterization Methods

Nitrogen sorption experiments were conducted using a Micromeritics ASAP 2010 at 77 K. Samples were degassed to 1 μm Hg at 100 °C prior to analysis. Standard methods were used for calculation of material characteristics. The Brunauer-Emmett-Teller (BET) method was used to determine surface area; the Barrett-Joyner-Halenda (BJH) method was used to calculate pore size from the adsorption branch of the isotherm; the single point method was used to calculate pore volume at relative pressure (P/P_0) 0.97.

Powder X-ray diffraction patterns were collected at room temperature using CuKα radiation from a Brüker MICROSTAR-H X-ray generator operated at 40 kV and 20 mA equipped with a 5 m Radian collimator, and a Brüker Platinum-135 CCD area detector. A custom fabricated beamstop was mounted on the detector to allow data collection to approximately 0.4° 2θ (approximately 210 Å) with a sample-to-detector distance of 30 cm. After unwarping the images, the XRD^2 plug-in was used to integrate the diffraction patterns from 0.3° to 8.4° 2θ.

Conducting carbon tape was used to mount samples for analysis by scanning electron microscopy (SEM). Gold sputter coating was accomplished under argon using a Cressington 108 auto sputter coater (duration 60 s). SEM images of the samples were obtained using a LEO 1455 SEM (Carl Zeiss SMT, Inc., Peabody, MA).

Morphological Characteristics

The morphological properties of the synthesized materials are summarized in Table 1. The MSN support material had surface area of 730 m^2/g with a pore volume of 0.75 cm^3/g. Nitrogen sorption characterization yielded a type IV isotherm with a steep increase in adsorption in the relative pressure range (ca 0.2–0.45), corresponding to capillary condensation in channel-type mesopores (Fig. 3A). Another adsorption increase was observed in the high pressure region near $P/P_0 = 1.0$, which may be due to textural porosity formed by aggregated nanoparticles or other larger mesopores [53]. The pore size distribution shows two peaks, with an average pore size of 50 Å (Fig. 3B). The particles are spherical with an average diameter of 96 nm (determined from SEM images, Fig. 4). The bare MSN materials (NS in Fig. 3) were functionalized with trehalose (NS-T), glucosamine (NS-G), and BSA (NS-B). Functionalization resulted in a loss in surface area for the NS-G and NS-T materials to 320 m^2/g with an accompanying loss in pore volume to 0.31 cm^3/g. Reductions in surface area and pore volume were greater upon BSA functionalization (166 m^2/g and 0.26 cm^3/g).

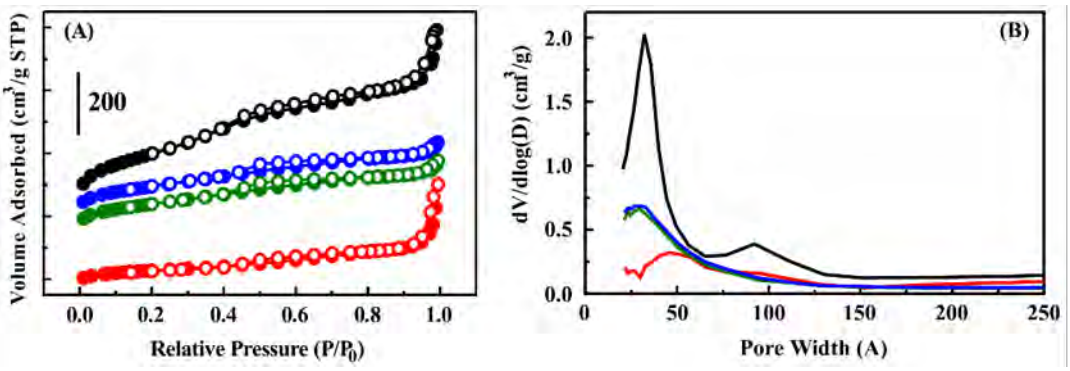

Fig. 3 — MSN materials. (A) Characterization of nanospherical silicate particles by nitrogen adsorption. (B) Pore size distributions. NS (black), NS-G (blue), NS-T (green), and NS-B (red). [66]

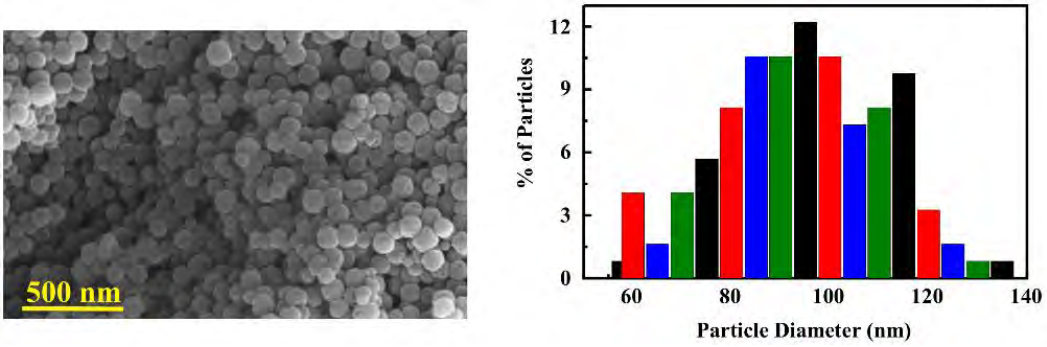

Fig. 4 — MSN materials. Characterization of nanospherical silicate particles using SEM imaging. Particle diameter distributions were determined based on these images. [66]

The sorbents with varied chemical functionalities also provided a range of morphological characteristics. Pore diameters for the materials ranged from 43 to 223 Å while the BET surface areas ranged from 140 to 1000 m^2/g. The chemical compositions of the sorbents provide a wide range of binding and interaction properties (Fig. 5). Diethylbenzene-bridged materials and those functionalized with pendent phenyl groups offer a somewhat hydrophobic environment as well as a high concentration of π-bonds (MM5, P5, P10; Fig. 6). The hydroxyl groups of these types of silicate materials tend to be acidic; incorporation of primary amine groups offers basic sites (N5; Fig. 7). The dendrimer modification (DEN) provides a greater number of basic sites at greater distance from the surface and increased hydrophobicity in the sorbent (Fig. 7). The alkylammonium functionalities offer cationic groups in two different material morphologies with relatively disordered (CF2M2B) and ordered (HX2M2B) mesopore structures (Fig. 8). The materials with ethylenediamine pendent groups (CuEDA and ZnEDA) offer sites for metal ion chelation (Fig. 9). The presence of cations is known to impact the secondary structure of DNA; the presence of copper has been shown to decrease DNA melting temperatures while zinc causes an increase [77].

Chitosan offers antimicrobial activity as well as the potential for multiple and complex cationic interactions with nucleic acids (Fig. 10). Two different approaches were used for generation of chitosan-modified sorbents. The first used physisorption of chitosan on a TEOS structure (ChTS). The second (ChMS) covalently incorporated the chitosan into the sorbent. Other multifunctional materials were

generated through combining stabilizing compounds with chemical functionalities. CF-B and CF-T combined the alkylammonium groups of the CF sorbent with covalently immobilized BSA and trehalose, respectively. CF-BT utilized adsorbed BSA and trehalose on the CF scaffold while CF-2X was synthesized through covalent immobilization of the two compounds.

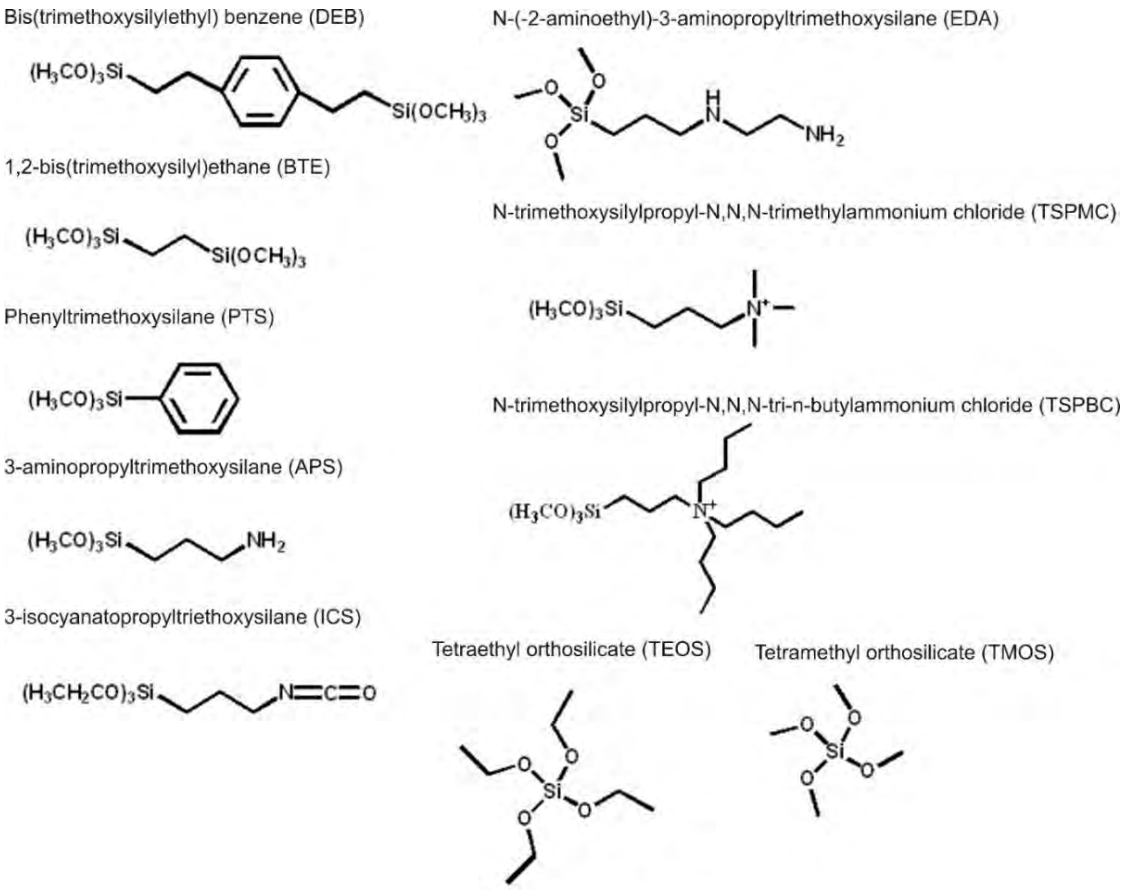

Fig. 5 — Precursor groups utilized in synthesis of sorbents

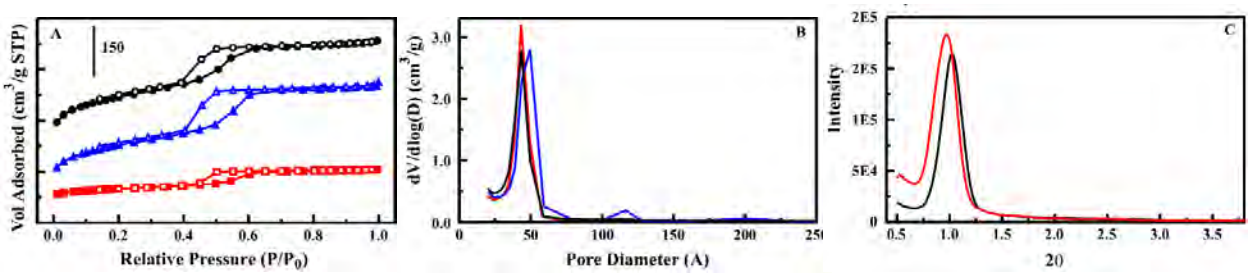

Fig. 6 — DEB-based sorbents. (A) Nitrogen sorption isotherms for MM5 (black); P10 (red); and P5 (blue). (B) Pore size distributions for materials (colored as in A). (C) The XRD spectra for MM5 (black) and P10 (red). The phenyl-incorporating materials, both 5% (470 m^2/g; 50 Å) and 10% (440 m^2/g; 43 Å), offer slightly less surface area than the 100% DEB sorbent (606 m^2/g; 44 Å) with comparable pore diameters. [78]

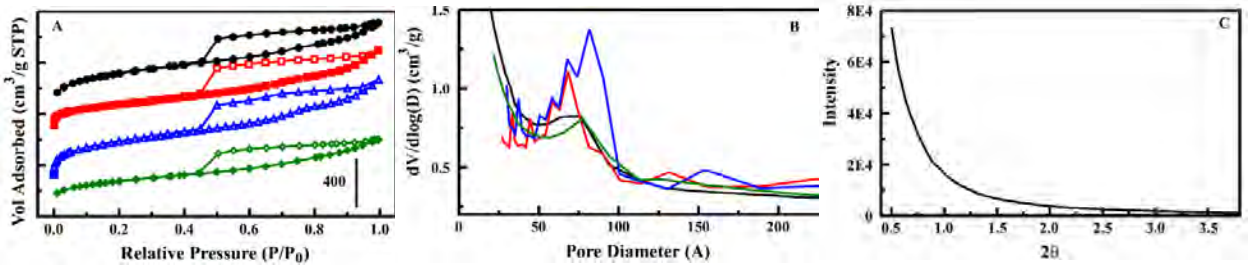

Fig. 7 — BTE-based sorbents. (A) Nitrogen sorption isotherms for the 100% BTE sorbent (black); N5 (red); the BTE sorbent with isocyanate groups (blue) and the DEN sorbent (green). (B) Pore size distributions for materials (colored as in A). (C) The XRD spectrum for the 100% BTE sorbent.

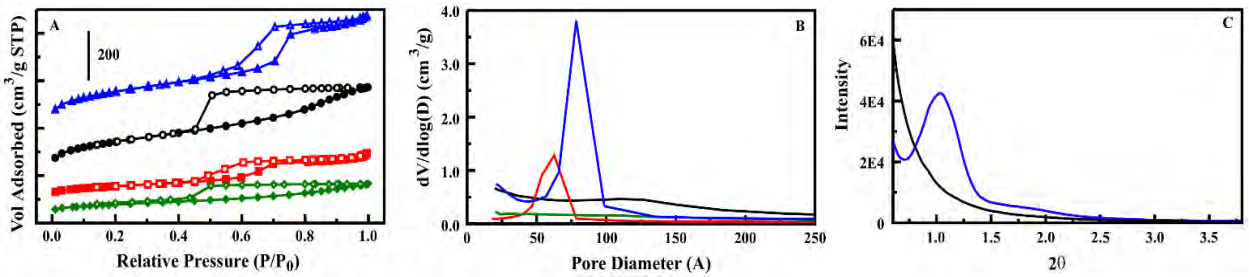

Fig. 8 — Alkyammonium-functionalized sorbents. (A) Nitrogen sorption isotherms for the base HX sorbent (blue, 566 m^2/g, 77 Å); HX2M2B (red, 169 m^2/g, 63 Å); the base CF sorbent (black, 523 m^2/g, 111 Å); and CF2M2B (green, 143 m^2/g, 93 Å). (B) Pore size distributions for materials (colored as in A). (C) The XRD spectrum for the base HX and CF sorbents. Functionalization of the HX and CF sorbents resulted in significant loss in surface area. Pore diameters for the functionalized materials were broadened and lacked a well-defined peak.

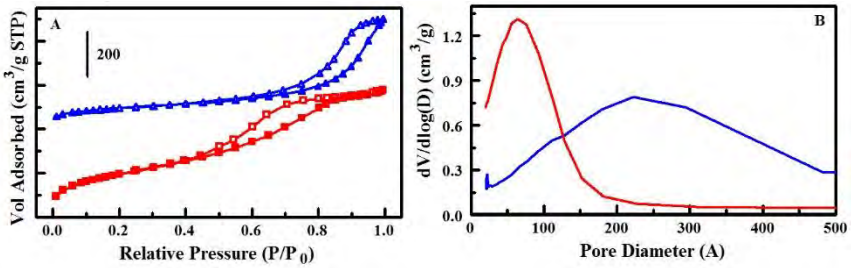

Fig. 9 — Metal-functionalized sorbents. (A) Nitrogen sorption isotherms for CuEDA (red) and ZnEDA (blue). (B) Pore size distributions for materials (colored as in A).

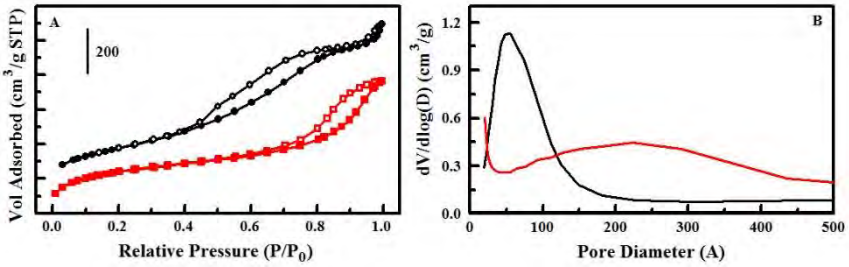

Fig. 10 — Chitosan-functionalized sorbents. (A) Nitrogen sorption isotherms for ChTS (black) and ChMS (red). (B) Pore size distributions for materials (colored as in A).

TARGET BINDING FROM AQUEOUS SOLUTION

RNA, DNA, and ssDNA Preparation

Triosephosphate isomerase (TIM, accession no. AF247559) of *Arabidopsis thaliana* was chosen as control RNA. TIM RNA transcripts were generated as previously described [66] from pSP64poly(A)-TIM linearized with EcoRI and *in vitro* transcribed from the SP6 promoter using the MEGAscript high-yield transcription kit (Life Technologies) according to the manufacturer's recommended protocol. *A. thaliana* NAC1 (accession no. AF198054) was chosen as control DNA and a 1059 nucleotide segment of the gene was PCR out of cDNAs of *A. thaliana* and cloned into TOPO4.0 vector (Life Technologies). The plasmid containing the NAC1 gene was used as a template for PCR with M13 primers, then digested with restriction enzymes PstI and XbaI (New England BioLabs, Inc., Ipswich, MA). This was then cloned into pSP64 polyA Vector (Promega Corporation, Madison, WI) digested with the same enzymes to generate pSP64poly(A)-NAC. NAC1 DNA was amplified by PCR with SP6 and M13R primers, and the PCR products were purified using a QIAquick PCR purification kit (Qiagen).

Single strand NAC1 DNA (ssNAC1) was generated based on the protocol developed by Tang et al. [79] with slight modification. Briefly, ssNAC1 was PCR amplified in 50 µL reaction volume containing 1x Green GoTaq® reaction buffer (Promega Corporation), 3 mM $MgCl_2$, 200 µM each of dNTPs, 20 nM each of SP6 and M13R primers, 375 nM of NAC1 forward primer, 1 unit of GoTaq® DNA polymerase (Promega Corporation), and 0.01 ng of pSP64poly(A)-NAC DNA. Reactions were performed with initial denaturation at 95 °C, 3 min, followed by 20 cycles of 95 °C, 20 s; 52 °C, 30 s; and 72 °C, 60 s; and 20 cycles 95 °C, 20 s; 58 °C, 30 s; and 72 °C, 60 s with final extension at 72 °C, 5 min. The ssNAC1 PCR products were confirmed using 1.5% TAE agarose gel, then purified using DNA Clean & Concentrator™-5 (Zymo Research) according to manufacturer's recommended protocol for ssDNA purification.

Nucleic Acid Adsorption and Elution Protocols

Adsorption of nucleic acids by the porous sorbents was performed as previously described [66]. Briefly, samples were vortexed, placed on an agitator, and incubated for 20 min. Following incubation, samples were centrifuged at 2000 rpm for 10 min and supernatants were separated from the precipitated sorbents.

During the course of this effort, the need for a preconditioning step was identified. When used, sorbents were washed prior to nucleic acid adsorption by centrifuging 0.3 mg of sorbent in 300 µL nuclease-free water at 1000 g for 10 min. The supernatant was removed, and the sorbent was resuspended in 300 µL of 10 mM Tris/1% Triton X-100 followed by incubation for 15 min at room temperature with agitation. The sorbents were again centrifuged at 1000 g for 10 min, and the supernatant was aspirated and discarded. The sorbents were then resuspended in 330 µL of 10 mM Tris/1% Triton X-100 for use in adsorption experiments as described above.

For stability testing, supernatants were separated from the precipitated sorbents, and the sorbents were left to dry at room temperature overnight. Control target samples were stored as prepared for adsorption experiments (in solution).

Nucleic acid elution was performed using 20 to 100 µL of different buffers at various temperatures as indicated in the text and figure captions. Sorbents with encapsulated NA were mixed with elution buffer and vortexed briefly, then incubated at the indicated temperature for 10 min. After incubation, the samples were centrifuged at 1000 g for 10 min; the supernatants were used for quantitative real-time reverse transcription PCR (qRT-PCR) or real-time PCR (qPCR).

Real-Time Reverse Transcription PCR and Real-Time PCR

The recovery rates of TIM RNA were quantified using qRT-PCR as previously described [66]. qRT-PCR was performed using iScript™ one-step RT-PCR kit (Bio-Rad Laboratories, Hercules, CA) with primers TIM134F (5'-CCGCCGTCTCCTCCCACCAA-3') and TIM252R (5'-TCCGGATCCAGCCATGGCAAC-3'). Eluted RNA (1 mL) was used as template for 25 mL RT-PCR reactions using MyiQ Thermal Cycler (Bio-Rad Laboratories). Serial dilutions (10×) of TIM RNA (1–10^5 fg/μL) were used as the standard curve. The qRT-PCR reactions were performed using the following conditions: 50 °C for 10 min, and 95 °C for 3 min 30 s, followed by 30 to 35 cycles of 10 s of denaturing at 95 °C; and 20 s of annealing/extension at 64 °C.

The recovery rates of NAC1 and ssNAC1 were quantified using qPCR. qPCR was performed using iQ SYBR® Green Supermix (Bio-Rad Laboratories) with primers NAC1-225F (5'-ATCGACCACCTCTTGTCCTG-3') and NAC1-377R (5'-CCGTTGCTCGGTTAGTTCTC-3'). Eluted NA (1 μL) was used as template for 25 μL PCR reactions using MyiQ Thermal Cycler (Bio-Rad Laboratories). A serial dilution of NAC1 DNA (10×; 1–10^5 fg/μL) was used as standard curve. The qPCR reactions were performed using the following conditions: 95 °C for 3 min, followed by 30 to 35 cycles of 10 s of denaturing at 95 °C, 10 s of annealing at 56 °C, and 10 s of extension at 72 °C.

Target Adsorption

Target adsorption was evaluated using a batch-wise approach with sacrificial samples. An example of single point data is provided in Fig. 11. Collections of this type of data were used to generate isotherms (see Table 2; Figs. 12 and 13). Equilibrium adsorption for all sorbents was reached within the first 10 min of contact with RNA-containing solutions. The Langmuir-Freundlich (LF) binding isotherm is a generalized form of the Langmuir model often applied to solid sorbents:

$$q = \frac{\frac{a}{m}k[L]^n}{1+k[L]^n} \tag{1}$$

This isotherm was applied to the data sets generated for target binding. Parameters were generated for each of the materials: an effective affinity constant for the target (k), the saturated loading capacity of the sorbent (q_s), and the site heterogeneity (n) within the sorbent based on the free ([L], ng) and bound (q, ng/μg) target. Here, the constant α divided by the mass (m) yields the more typically utilized saturation capacity (q_s) for the model [68,80,81].

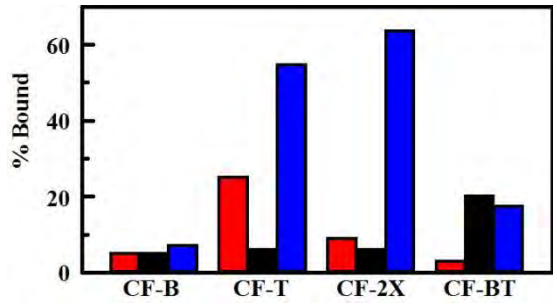

Fig. 11 — Nucleic acid targets bound from solutions consisting of 30 µg sorbent (CF variants) with 300 ng of TIM RNA (red); 3 ng NAC1 DNA (black); or 30 ng NAC1 ssDNA (blue).

Table 2 — Langmuir Isotherm Parameters for RNA, DNA, and ssDNA Binding by Unwashed Sorbents

	RNA				DNA				ssDNA			
Material	**α (ng/µg • µg)**	**k (ng^{-1}) ×10^3**	**Chi^2**	**Std. Error**	**α (ng/µg • µg)**	**k (ng^{-1}) ×10^3**	**Chi^2**	**Std. Error**	**α (ng/µg • µg)**	**k (ng^{-1}) ×10^3**	**Chi^2**	**Std. Error**
Unwashed Sorbents												
NS	410	550	--	--								
NS-T	408	550	--	--								
NS-G	204	73	--	--								
NS-B	438	130	--	--								
N5	165	46.7	381	3.45	1530	38.3	105	4.81	75.7	4.72	136	1.39
P5	204	6.91	691	3.91	9.14	0.661	187	6.34	62.6	0.512	25.7	0.607
P10	104	7.92	552	3.50	9.26	0.698	561	9.71	38.2	0.478	45.9	0.810
CuEDA	690	6.03	2920	7.09	118	8.53	852	4.33	147	1.12	407	2.41
ZnEDA	301	1.95	234	2.26	55.8	4.14	422	10.5	104	0.707	75.4	1.14
MM5	97.6	17.7	200	2.08	9.13	0.614	110	1.33	57.6	177	200	2.08
HX2M2B	375	8.18	1421	4.95	114	8.27	60.3	3.62	256	1.78	327	2.67
CF2M2B	571	9.18	3580	8.83	26.2	1.91	118	1.60	158	1.06	141	1.83
DEN	279	31.8	960	5.73	N/A†	N/A	N/A	N/A	94.8	0.563	634	3.71
ChTS	255	42.9	1520	5.75	N/A†	N/A	N/A	N/A	7.43	0.467	5.64	0.284

†Insufficient data for generation of an isotherm; DEN ~100% bound, ChTS ~0% bound.

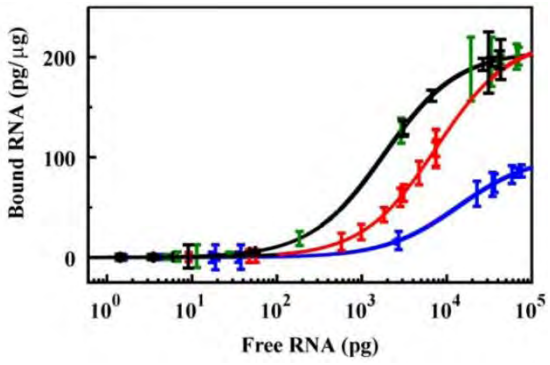

Fig. 12 — Binding of RNA. Binding isotherms for NS (black line, black symbols), NS-T (black line, green symbols), NS-G (blue), and NS-B (red) determined based on results of RT-PCR. Error bars are the standard deviation in the measurements.

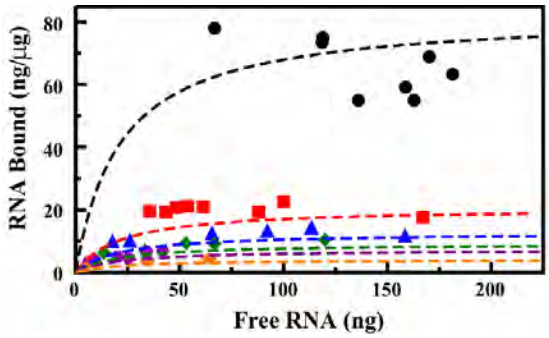

Fig. 13 — Binding isotherm. RNA bound by the N5 sorbent without prewashing. Here, sorbent masses of 2 μg (black circle), 8 μg (red square), 13 μg (blue triangle), 18 μg (green diamond), 23 μg (purple hexagon), and 40 μg (orange star) were utilized for capture of RNA from a 240 μL solution containing ~300 ng TIM RNA target.

Differences in adsorption of RNA by the NS and NS-T materials were within the noise of the measurements (Fig. 12). Fitting of the data sets using the LF binding isotherm indicated a saturation capacity of 410 ng/μg for the NS and NS-T materials. The saturation capacity for NS-B was similar at 438 ng/μg and slightly less for NS-G at 204 ng/μg. Affinity constants for NS and NS-T (0.55 ng^{-1}) were greater than those determined for NS-B (0.13 ng^{-1}) and NS-G (0.07 ng^{-1}). Fits of the data indicated homogeneous interaction sites within the sorbents (n = 1 in all cases).

The parameters obtained using this approach indicate the maximum target that can be bound (α) and the rate at which that limit will be approached (k). Based on this analysis, the RNA saturated loading limit for HX2M2B is greater than that of N5, but, at low free RNA concentrations, N5 will bind more target than HX2M2B (k = 0.0467 ng^{-1} versus 0.00818 ng^{-1}). N5 provided the greatest saturated loading limit for DNA, while HX2M2B provided the greatest limit for ssDNA. MM5, P5, and P10 showed moderate to low total binding and affinity for all three targets. DEN performed moderately for RNA and ssDNA and bound by far the greatest amount of DNA. CuEDA and ZnEDA performed moderately for DNA and ssDNA, but CuEDA provided the greatest RNA saturated loading limit.

ELUTION OF BOUND TARGETS

Initial evaluations assessed recovery of RNA from the NS material variants using EB buffer (10 mM Tris-Cl, pH 8.5) at room temperature. Recovery of RNA from NS-B (~1%) was lower than that for any of the other sorbents (5%–18%; Fig. 14A). In an attempt to improve this recovery rate, various elution solutions and temperatures were evaluated. Because NS-B yielded the poorest RNA recovery, it was used as the model material for these studies. NEB RNA elution buffer (20 mM Tris-Cl, pH 7.5, 1 mM EDTA) (New England BioLabs, Inc.) and nuclease-free water were selected as eluent solutions in addition to the EB elution buffer. Results indicated that recovery of RNA in nuclease-free water was comparable to that in EB buffer (~1%). Increasing the incubation temperature to 65 °C improved the recovery rate (~2%), and heating nuclease-free water to 95 °C improved the recovery rate further (~10%). Increased incubation temperature similarly improved the recovery rate for EB buffer. The most effective recovery was achieved using NEB RNA elution buffer at 50 °C (63%; Fig. 14B) [66].

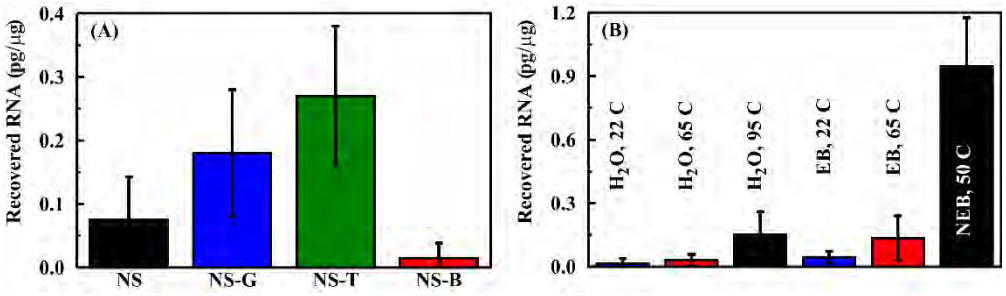

Fig. 14 — Recovery of RNA adsorbed by sorbents (NS variants). (A) Recovery of RNA from sorbents using EB buffer for elution at room temperature (22 °C). Total applied target for these studies was 1.5 pg/mg. (B) Recovery of RNA from NS-B using varied eluents at different temperatures. Values indicate the percentage of the total target bound that was recovered in the elution step. [66]

Elution of bound target from the sorbents bearing chemical functionalities was also evaluated. Initial attempts at recovering RNA using EB buffer at 50 °C provided minimal return from these materials. NEB buffer provided the best performance for the NS sorbents, but did not offer target recovery from these materials. Variations on temperature, volume, incubation period, and detergent concentrations were considered and tested, as was the inclusion of solvent and sodium chloride [82,83]. Other studies have indicated the impact of buffer pH on the elution efficiency related to silicate materials [84–86]; however, varying pH (5.7 to 8.0) did not have an impact on RNA recovery. It has been argued that nucleic acid interactions with silicate materials are via amine and carboxyl groups [86]. Methods used to displace these interactions, as well as those used to displace RNA from negatively charged membranes [87], were considered and tested without improvement. Finally, various nucleic acid washing solutions and hybridization buffers were evaluated without success (less than 1% of target recovered). Table 3 lists the solutions tested.

Table 3 — Elution Solutions and Conditions Evaluated

Solution	Volume (µL)	Time (h)	Temp. (°C)
EB buffer (10 mM Tris-Cl, pH 8.5)	20, 50, 200	0.3, 3	50
EB buffer (10 mM Tris-Cl, pH 8.5) with 0.1% Tween 20	50	0.3	50
EB buffer (10 mM Tris-Cl, pH 8.5) with 0.1% SDS	50	03	50
EB buffer (10 mM Tris-Cl, pH 8.5) with 0.1% SDS and Tween 20	50	0.3	50
Nuclease-free water	20, 50, 200	0.3, 3	RT, 65, 95
1x GoTaq PCR buffer (Promega) with 0.1% SDS	20, 100, 200	0.3, 3	50
NEB buffer	50	0.3	50
NEB buffer with 0.1% SDS	50, 100	0.3	50
50 mM sodium phosphate buffer pH 5.7 to 8.0	50	0.3, 5	50
50 mM sodium phosphate buffer with 0.1% Tween 20, pH 7.2	50	0.3	50
10, 50, 100, 200, or 250 mM Tris pH 8.0	50, 100, 200	0.3	50
10, 100, or 200 mM Tris with 20% ethanol	100	0.3	50
10 mM Tris with 50, 100, 150, or 200 mM NaCl pH 8.0	50, 100, 200	0.3	50
10 mM Tris with 1, 5, or 10% Triton X100 pH 8.0	50	0.3	50
10 mM Tris with 100 mM NaCl and 0.1% SDS	100	0.3	50
10 mM Tris with 100 mM NaCl and 1% Triton X-100	100	0.3	50
25 mM Tris with 250 mM glycine pH 8.0 or 7.0	100	0.3	50
25 mM Tris with 250 mM glycine and 0.1% SDS pH 8.0 or 7.0	100	0.3	50
25 mM Tris with 250 mM glycine and 1% Triton X-100	100	0.3	50
100 mM Tris with 50 mM glycine pH 8.0 or 9.5	100	0.3	50
100 mM Tris with 50 mM glycine and 0.1% SDS pH 9.5	100	0.3	50
100 mM Tris with 50 mM glycine and 1% Triton X-100 pH 8.0	100	0.3	50
100 or 200 mM Tris with 0.1% SDS pH 8.0	100	0.3	50
200 mM Tris with 50 or 100 mM NaCl pH 8.0	50, 100	0.3	50
200 mM Tris with 100 mM NaCl and 20% ethanol, pH 8.0	100	0.3	50
200 mM Tris with 0.1% SDS and 20% ethanol, pH 8.0	100	0.3	50
200 mM Tris with 0.1% SDS, pH 8.0	100	0.3	50
Hyb buffer (MiSeq)	100	0.3	50
Hyb buffer (Affymetrix)	100	0.3	50
0.2X or 2X SSC with 0.1% SDS	100	0.3	50
0.6X or 6X SSPE with 0.1% SDS	100	0.3	50
0.31, 0.63, 1.3, or 2.5 M NaCl	100	0.3	50
50 mM glycine with 150 mM NaCl pH 9.5	100	0.3	50
50 mM glycine with 150 mM NaCl and 0.1% SDS pH 9.5	100	0.3	50
1xTAE with 0.1% SDS	100	0.3	50

(Table continues)

Table 3 (cont.) — Elution Solutions and Conditions Evaluated

Solution	Volume (µL)	Time (h)	Temp. (°C)
Washed Sorbents			
10 mM Tris pH 8.0	100	0.3	50
10 mM Tris with 20% ethanol	100	0.3	50
100 mM Tris with 0.1% SDS	100	0.3	50
10 mM Tris with 100 mM NaCl	100	0.3	50
NEB with 0.1% SDS	100	0.3	50
Washed DEN Sorbent			
1x PCR 0.1% SDS	100	0.3	50
NEB with 0.1% SDS			
10 mM Tris pH 8.0	100	0.3	50
10 mM Tris with 20% ethanol	100	0.3	50
10 mM Tris with 100 mM NaCl	100	0.3	50
10 mM Tris with 100 mM NaCl and 0.1% SDS	100	0.3	50
10 mM Tris with 100 mM NaCl and 1% Triton X-100	100	0.3	50
25 mM Tris with 250 mM glycine and 0.1% SDS	100	0.3	50
25 mM Tris with 250 mM glycine and 1% Triton X-100	100	0.3	50
100 mM Tris with 0.1% SDS	100	0.3	50
100 mM Tris with 50 mM glycine and 0.1% SDS	100	0.3	50
100 mM Tris with 50 mM glycine and 1% Triton X-100	100	0.3	50
0.6X SSPE with 0.1% SDS	100	0.3	50
0.6X SSPE with 1% Triton X-100	100	0.3	50

Based on previous experience and other materials used for nucleic acid hybridization, a preconditioning step was evaluated for the sorbents. This type of prehybridization step has been used in Northern and Southern blotting technologies to reduce nonspecific binding of nucleic acids [88]. Here, the procedure involved incubating the sorbent in 10 mM Tris with 1% Triton X-100 for 15 min at room temperature prior to target adsorption. Figure 15 provides single point data on target binding by the washed N5, CuEDA, HX2M2B, CF2M2B, DEN, and ChTS. ChMS bound 100% of all three targets. Other sorbents bound less than 5% of all three targets. This preconditioning step strongly impacted the binding behavior of the sorbents and led to less error in the resulting fits (Fig. 16; Table 4). ZnEDA offered lower saturated loading capacities than CuEDA prior to washing and likely lost binding capacity upon interaction with the Triton X-100 as observed for CuEDA. This surfactant would also be expected to interact with the surfaces of the MM5, P5, and P10 sorbents given their somewhat hydrophobic nature and the available π-interaction sites. Other prehybridization solutions, such as 2X SSC (0.3 M sodium chloride with 30 mM trisodium citrate at pH 7) with 0.1% SDS or 6X SSPE (900 mM NaCl with 60 mM sodium phosphate and 6 mM ethylenediaminetetraacetic acid) with 0.1% SDS, could be considered for use with these sorbents.

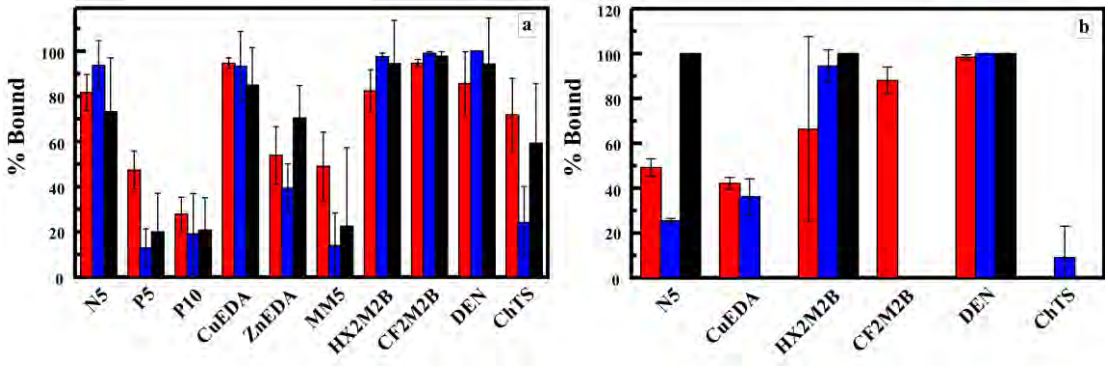

Fig. 15 — Nucleic acid targets bound from solutions consisting of 30 µg sorbent with 300 ng of TIM RNA (red); 3 ng NAC1 DNA (blue); or 30 ng NAC1 ssDNA (black) using sorbents without preconditioning (a) and following the preconditioning step (b). Error bars indicate standard deviation across six measurements.

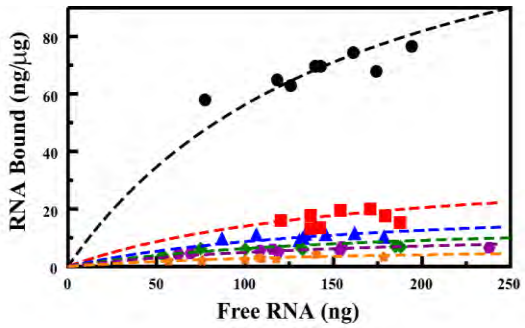

Fig. 16 — Binding isotherms. RNA bound by the N5 sorbent following the described preconditioning step. Here, sorbent masses of 2 µg (black circle), 8 µg (red square), 13 µg (blue triangle), 18 µg (green diamond), 23 µg (purple hexagon), and 40 µg (orange star) were utilized for capture of RNA from a 240 µL solution containing ~300 ng TIM RNA target. (Compare to Fig. 13 results without the preconditioning step.)

Table 4 — Langmuir Isotherm Parameters for RNA, DNA, and ssDNA Binding by Washed Sorbents

	RNA				DNA				ssDNA			
Material	**α (ng/µg • µg)**	**k (ng^{-1}) ×10^3**	**Chi^2**	**St. Error**	**α (ng/µg • µg)**	**k (ng^{-1}) ×10^3**	**Chi^2**	**St. Error**	**α (ng/µg • µg)**	**k (ng^{-1}) ×10^3**	**Chi^2**	**St. Error**
Washed Sorbents												
N5	300	6.13	124	1.64	61.4	4.48	1315	8.48	157	1.10	41.7	0.952
CuEDA	167	30.2	924	3.60	60.6	4.41	905	6.17	N/A†	N/A	N/A	N/A
HX2M2B	220	82.1	247	2.06	8.78	0563	344	11.1	113	0.728	16.4	0.604
DEN	165	202	1260	3.35	184	13.3	213	6.81	176	1.22	90.4	1.43
ChMS	450	930	456	2.93	19.6	19.6	308	2.5	630	0.93	19.5	0.606

†Insufficient data for generation of an isotherm; CuEDA ~0% bound.

Elution of bound targets from the preconditioned sorbents was evaluated, again testing different elution solutions. Figure 17 shows nucleic acid recovery results for four sorbents using five different solutions. RNA recovery (Fig. 17a) was significantly increased from less than 1% in the unwashed sorbents to between 20% and 80% using 100 mM Tris with 0.1% SDS for HX2M2B, N5, and CuEDA. Recovery of DNA and ssDNA (Fig. 17b, 17c) was also improved following the preconditioning step, with a small amount of DNA recovered from even the DEN sorbent (Fig. 17b, black). For ChMS (not shown), RNA recovery was improved to 15%; however, less than 2% of DNA and ssDNA could be recovered.

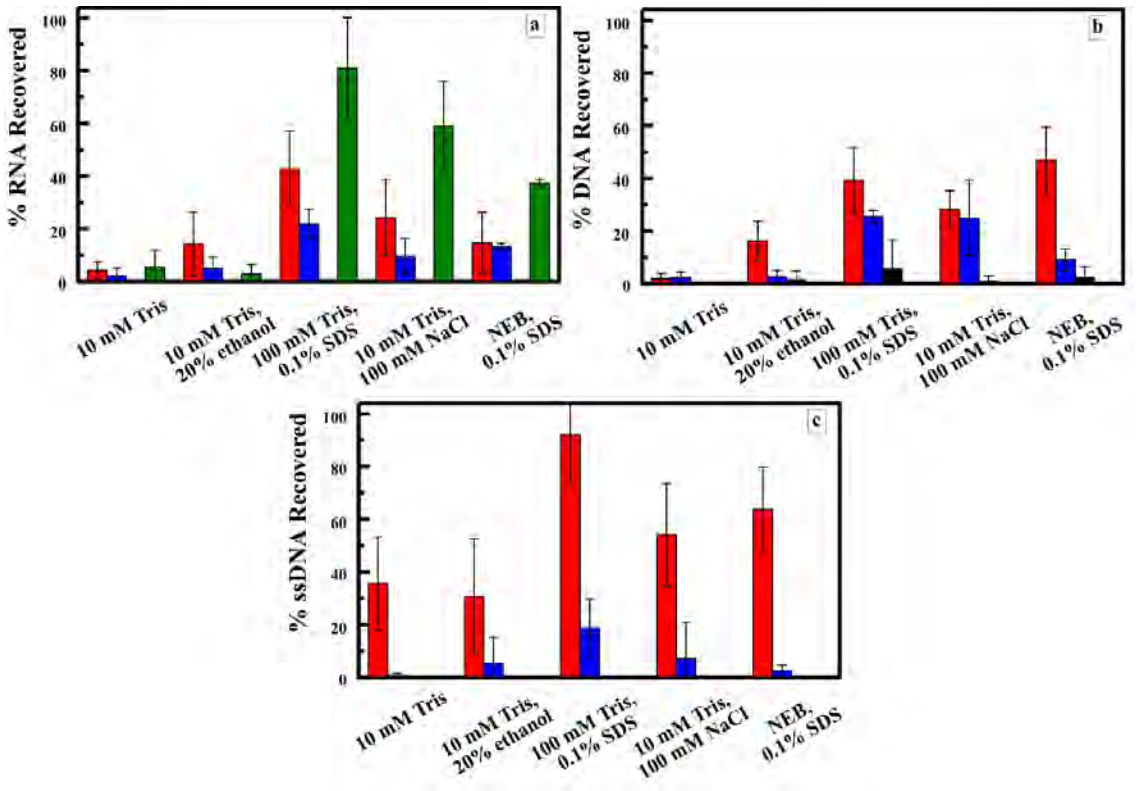

Fig. 17 — Elution. Nucleic acid targets eluted from washed sorbent materials reported as a percentage of the target initially adsorbed: N5 (red); HX2M2B (blue); DEN (black); CuEDA (green). All elution solutions utilized 100 μL at 50 °C for 20 min: RNA (a), DNA (b), and ssDNA (c).

STABILITY

To evaluate the potential of the sorbents to enhance the stability of stored NA targets, a large batch sample of target adsorbed on material was prepared. The sample was then divided into aliquots, and the supernatants were separated from the precipitated sorbents. A control sample consisting of the target only in solution was retained for comparison. No special protection from light or control of humidity was employed. Retained RNA from that initially adsorbed onto the sorbents was evaluated over a period of 16 months during storage at 4 °C. Because these studies were initiated prior to completion of studies on varied elution conditions, extraction of the RNA into EB buffer at room temperature was utilized. The supernatant was removed from the samples, but they were not dried; adsorbed RNA on the sorbents was stored in the presence of residual water. Figure 18 shows RNA recovery results. Early results (53 days) indicated improved stability in all functionalized sorbent materials over that in the bare NS sorbent. After 81 days, however, the differences between the NS, NS-B, and NS-T materials became less significant. The NS-G sorbent consistently retained more RNA than the other sorbents through 260 days. At one year, all sorbents showed similar RNA retention at 2 orders of magnitude less than that recovered on day 1.

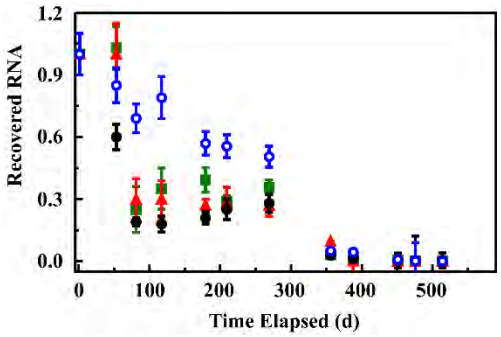

Fig. 18 — Recovery of RNA adsorbed onto sorbents following storage at 4 °C. Data is presented as the ratio of the RNA recovered on a given day to that recovered for the same sorbent on day 1 of the experiment. Recovery of RNA from NS (black), NS-G (blue), NS-T (green), and NS-B (red) sorbents.

Stability was also evaluated for N5, HX2M2B, and DEN sorbents. In this case, aliquots were allowed to dry at room temperature overnight prior to storage. The sorbents were sampled during 200 days of storage either at room temperature or at 37 °C. Over the course of the experiments, room temperature varied between 18 and 23 °C while relative humidity ranged from 42% to 61%. Figure 19 presents RNA results; Fig. 20 presents DNA results; and Fig. 21 presents ssDNA results. The recovered target is normalized to the amount recovered on day 1 of the experiment. Over this period at room temperature, RNA eluted from N5 (red) gradually decreased to 20% of the day 1 recovery while that from HX2M2B (blue) decreased to 5%. Recovery from DEN (green), significantly lower on day 1, decreased to less than 10% by day 80. RNA in the control sample drops to less than 10% by day 29. At 37 °C, recovery of RNA from all three materials was increased as compared to that from the control sample. More than 20% was recovered from N5 through day 140, from HX2M2B through day 80, and from DEN through day 50. These results indicate that the three sorbents offer improvements in RNA stability both at room temperature and at 37 °C.

The decrease in DNA recovered from N5 and HX2M2B at room temperature and at 37 °C was similar to the decrease in the DNA content of the control sample (Fig. 20). For ssDNA, on the other hand (Fig. 21), while the control sample at room temperature dropped below 20% of the original content on day 121,

recovery from N5 remained above 20% beyond day 170. When stored at 37 °C, however, the decrease in ssDNA recovered from N5 was similar to that of the control sample. While the decrease in ssDNA recovered from HX2M2B at room temperature was similar to the decrease in the ssDNA content of the control sample, HX2M2B showed slightly improved recovery of ssDNA over the first 20 days at 37 °C. Results with DEN showed more rapidly decreasing DNA and ssDNA content than that observed for the control samples.

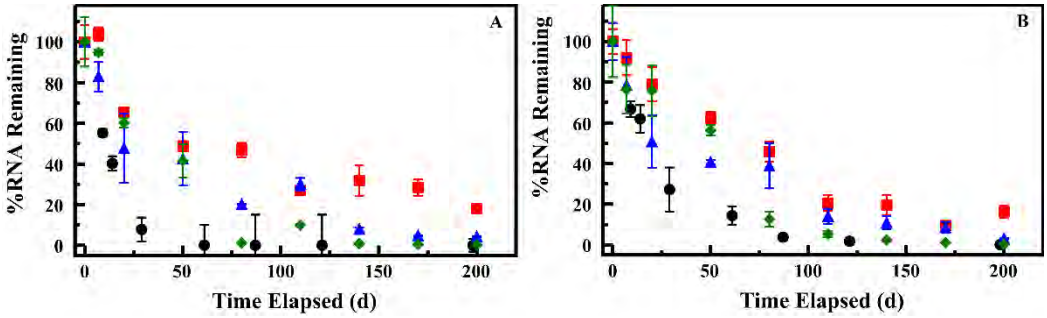

Fig. 19 — Stability of RNA. RNA recovered from N5 (red square), HX2M2B (blue triangle), and DEN (green diamond) following storage at room temperature (A) and at 37 °C (B). Data for similarly stored sample of target only in solution (black circle) is provided for comparison.

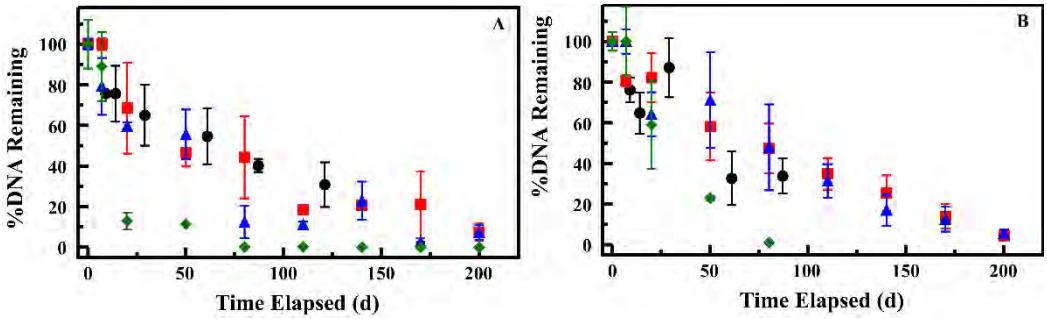

Fig. 20 — Stability of DNA. DNA recovered from N5 (red square), HX2M2B (blue triangle), and DEN (green diamond) following storage at room temperature (A) and at 37 °C (B). Data for similarly stored sample of target only in solution (black circle) is provided for comparison.

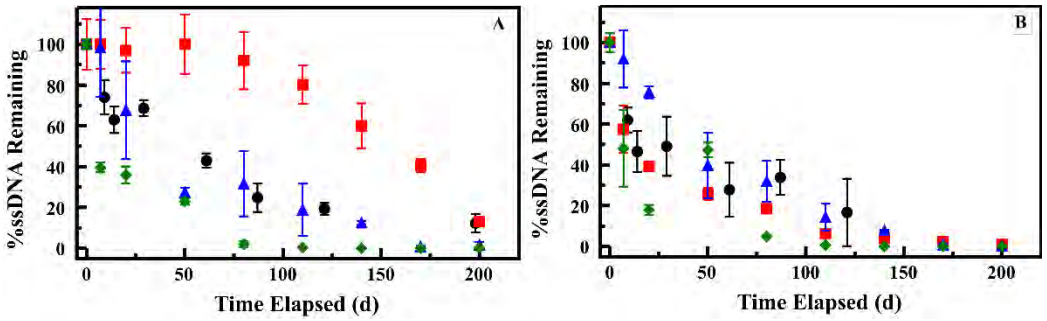

Fig. 21 — Stability of ssDNA. ssDNA recovered from N5 (red square), HX2M2B (blue triangle), and DEN (green diamond) following storage at room temperature (A) and at 37 °C (B). Data for similarly stored sample of target only in solution (black circle) is provided for comparison.

CAPTURE FROM COMPLEX SOLUTIONS

Escherichia coli was used to prepare samples for evaluation of nucleic acid target binding from complex solution. *E. coli* was streaked from glycerol stock onto LB agar plate and incubated overnight at 37 °C. A single colony was picked from the plate and grown in 5 mL LB broth overnight at 37 °C; this was used to inoculate 50 mL LB broth. OD_{600} was measured every hour after inoculation, and 1.5 mL of cells were aliquoted into 1.5 mL Eppendorf tubes and stored at 4 °C until ready to use. Bacteria cells were pelleted by centrifuge at 5000g for 10 min; supernatant was discarded; and pellets were subjected to various lysis conditions.

Bacterial Lysis

Genomic DNA was extracted from a sample using MasterPure™ Complete DNA and RNA Purification Kit (Epicentre) for use as a control and for generation of a standard curve. Lysis buffer/conditions were identified based on published protocols:

1. Bacteria was resuspended in Tris-EDTA buffer (100 μL; 30 mM Tris, pH 8.0 and 1 mM EDTA) with 5 mg/mL lysozyme and 1 μL proteinase K. The mixture was incubated at room temperature for 10 min. A microcentrifuge was used to spin down cell debris (maximum speed for 2 min). The supernatant containing genomic DNA was transferred to a new Eppendorf tube for OD and qPCR assessment.
2. Similar to protocol of 1 without proteinase K.
3. Same composition as 1. Following incubation, Buffer RLT was added to the mixture prior to centrifugation.
4. Same composition as 1. Following incubation, cells were subjected to three freeze and thaw cycles prior to centrifugation.
5. Similar to protocol of 4 without proteinase K.
6. Bacteria was resuspended in Tris-NaCl buffer (100 μL; 50 mM Tris, pH 8.0 and 150 mM NaCl) with 0.4 mg/mL lysozyme. The mixture was subjected to three freeze and thaw cycles. A microcentrifuge was used to spin down cell debris (maximum speed for 10 min). The supernatant containing genomic DNA was transferred to a new Eppendorf tube for OD and qPCR assessment.
7. Similar to 6 without lysozyme in the buffer.
8. Bacteria was resuspended in 100 μL of Tris-Triton (100 mM Tris, pH 8.0 and 2% Triton X-100) buffer with 10 mg/mL lysozyme. The mixture was incubated at room temperature for 10 min. A microcentrifuge was used to spin down cell debris (maximum speed for 2 min). The supernatant containing genomic DNA was transferred to a new Eppendorf tube for OD and qPCR assessment.
9. Similar to protocol of 8 without lysozyme in the buffer.
10. Bacteria was resuspended in PBS/EDTA/Triton buffer (100 μL; 0.5X PBS, 1 mM EDTA, 0.1% Triton X-100) with 10 mg/mL lysozyme. The mixture was subjected to three freeze and thaw cycles. A microcentrifuge was used to spin down cell debris (maximum speed for 10 min). The supernatant containing genomic DNA was transferred to a new Eppendorf tube for OD and qPCR assessment.
11. Similar to protocol of 10 with no lysozyme in the buffer.

12. Bacteria was resuspended in buffer P1 (Qiagen; 50 µL) and mixed with buffer P2 (Qiagen; 50 µL). Buffer N3 (Qiagen; 70 µL) was added and the solution was inverted to mix. A microcentrifuge was used to spin down cell debris (maximum speed for 10 min). The supernatant containing genomic DNA was transferred to a new Eppendorf tube for OD and qPCR assessment.
13. Bacteria was resuspended in Tris-sucrose (50 µL; 25 mM Tris, pH 8.0 and 20% w/v sucrose) with 20 mg/mL lysozyme (5 µL) and incubated on ice for 5 min. EDTA (5 µL; 0.5 M) was added followed by lysis buffer (50 µL; 50 mM Tris, pH 8.0 and 25 mM EDTA, 2% Triton X-100). The solution was incubated at room temperature for 15 min. A microcentrifuge was used to spin down cell debris (maximum speed for 10 min). The supernatant containing genomic DNA was transferred to a new Eppendorf tube for OD and qPCR assessment.

DNA concentrations were measured using Nanodrop 2000 (Thermo Scientific) to assess the 260/280 ratios. A stock solution (40 ng/µL) was prepared based on the OD reading and used for qPCR assessment. qPCR was performed using primers designed to target DNA polymerase III delta prime subunit (HolB) of *E. coli*. Based on OD readings and qPCR results, the PBS/EDTA/Triton buffer was selected for testing the performance of sorbents for adsorption and elution of targets.

Target Adsorption

Based on the performance of the sorbents as described above in the sections focused on adsorption, elution, and stabilization, the N5 and CuEDA sorbents were selected for the initial demonstration of capture from a complex solution. Figure 22 shows the DNA bound from the lysis solution using the two materials, as well as the amount recovered from them. Both sorbents bound significant percentages of the total DNA available (N5 100% at 100 µg). Recovery of target in this study was negatively impacted by the use of large sorbent concentrations in small volumes of eluent (100 µg in 100 µL; 100 mM Tris/0.1% SDS). Additional work, as well as the results presented above, indicate that a significant portion of the DNA should be recovered under more optimal conditions.

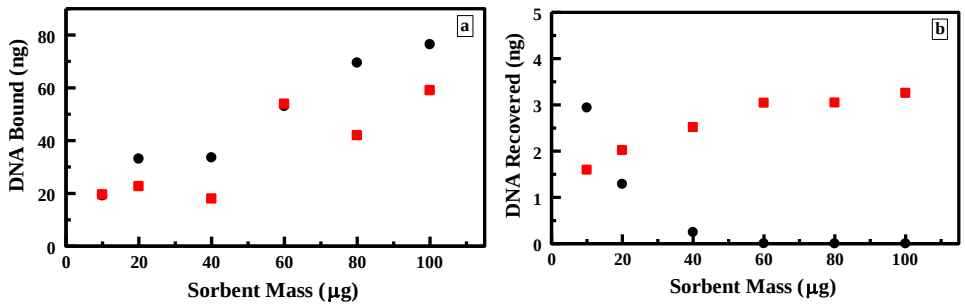

Fig. 22 — Binding and recovery of DNA. DNA (a) bound by and (b) recovered from N5 (black circle) and CuEDA (red square) from bacterial lysis solution.

CONCLUSIONS

Sorbent materials of the type described here provide capture and stabilization of nucleic acids using a single material. Capture and stabilization can be accomplished from complex solutions, eliminating the need for purification steps. The sorbents can incorporate a combination of stabilization compounds that are covalently linked to the sorbent. In this way, the compounds provide the necessary stabilization without causing downstream contamination for follow-on applications, and with no loss of stabilizing compounds regardless of the complexity of the matrix in which they are used. These sorbent materials are reusable.

Existing approaches focus on stabilization of purified nucleic acids, or on purification or extraction of these targets without addressing stabilization, especially that suitable to austere field environments. The materials and methods described here provide both extraction of the nucleic acid targets and stabilization of those nucleic acid materials for storage and shipment in the absence of refrigeration, using a single sorbent.

ACKNOWLEDGMENTS

Anthony P. Malanoski provided theoretical and computational support to this effort. Jenna R. Taft (formerly NOVA Research, Inc.) contributed to materials synthesis and morphological characterization. Michael A. Dinderman (formerly NRL, Code 6930) provided SEM/TEM analysis. Jeffrey R. Deschamps (NRL, Code 6930) and Syed B. Qadri (NRL, Code 6366) provided assistance with X-ray diffraction measurements. We thank Dr. Tomasz A. Leski for providing *A. thaliana* TIM RNA. Student contributors to this effort included Genevieve M. Haas of Northern Michigan University and Miles K.J. McConner of Norfolk State University.

REFERENCES

1. C. Frippiat, S. Zorbo, D. Leonard, A. Marcotte, M. Chaput, C. Aelbrecht, and F. Noel, "Evaluation of Novel Forensic DNA Storage Methodologies," *Forensic Science International: Genetics* **5**, 386–392 (2011).

2. M. Shabihkhani, G.M. Lucey, B.W. Wei, S. Mareninov, J.J. Lou, H.V. Vinters, E.J. Singer, T.F. Cloughesy, and W.H. Yong, "The Procurement, Storage, and Quality Assurance of Frozen Blood and Tissue Biospecimens in Pathology, Biorepository, and Biobank Settings," *Clinical Biochemistry* **47**, 258–266 (2014).

3. J.A. Blow, C.N. Mores, J. Dyer, and D.J. Dohm, "Viral Nucleic Acid Stabilization by RNA Extraction Reagent," *Journal of Virological Methods* **150**, 41–44 (2008).

4. A.H. Garcia, "Anhydrobiosis in Bacteria: From Physiology to Applications," *Journal of Biosciences* **36**, 939–950 (2011).

5. W. Block, R.I.L. Smith, and A.D. Kennedy, "Strategies of Survival and Resource Exploitation in the Antarctic Fellfield Ecosystem," *Biological Reviews* **84**, 449–484 (2009).

6. D. Clermont, S. Santoni, S. Saker, M. Gomard, E. Gardais, and C. Bizet, "Assessment of DNA Encapsulation, a New Room-Temperature DNA Storage Method," *Biopreservation and Biobanking* **12**, 176–183 (2014).

7. J. Bonnet, M. Colotte, D. Coudy, V. Couallier, J. Portier, B. Morin, and S. Tuffet, "Chain and Conformation Stability of Solid-State DNA: Implications for Room Temperature Storage," *Nucleic Acids Research* **38**, 1531–1546 (2010).

8. C. Brus, E. Kleemann, A. Aigner, F. Czubayko, and T. Kissel, "Stabilization of Oligonucleotide-Polyethylenimine Complexes by Freeze-Drying: Physicochemical and Biological Characterization," *Journal of Controlled Release* **95**, 119–131 (2004).

9. J.-H.S. Kuo and R. Hwang, "Preparation of DNA Dry Powder for Non-Viral Gene Delivery by Spray-Freeze Drying: Effect of Protective Agents (Polyethyleneimine and Sugars) on the Stability of DNA," *Journal of Pharmacy and Pharmacology* **56**, 27–33 (2004).

10. G.E. Hernandez, T.S. Mondala, and S.R. Head, "Assessing a Novel Room-Temperature RNA Storage Medium for Compatibility in Microarray Gene Expression Analysis," *Biotechniques* **47**, 667–670 (2009).

11. W. Li and F.C. Szoka, Jr., "Lipid-based Nanoparticles for Nucleic Acid Delivery," *Pharmaceutical Research* **24**, 438–449 (2007).

12. E. Wan, M. Akana, J. Pons, J. Chen, S. Musone, P.-Y. Kwok, and W. Liao, "Green Technologies for Room Temperature Nucleic Acid Storage," *Current Issues in Molecular Biology* **12**, 135–141 (2010).

13. C.L. Michaud and D.R. Foran, "Simplified Field Preservation of Tissues for Subsequent DNA Analyses," *Journal of Forensic Sciences* **56**, 846–852 (2011).

14. G. Seutin, B.N. White, and P.T. Boag, "Preservation of Avian Blood and Tissue Samples for DNA Analysis," *Can. J. Zool.-Rev. Can. Zool.* **69**, 82–90 (1991).

15. A. Allen-Hall and D. McNevin, "Human Tissue Preservation for Disaster Victim Identification (DVI) in Tropical Climates," *Forensic Science International: Genetics* **6**, 653–657 (2012).

16. A.J. Rissanen, E. Kurhela, T. Aho, T. Oittinen, and M. Tiirola, "Storage of Environmental Samples for Guaranteeing Nucleic Acid Yields for Molecular Microbiological Studies," *Applied Microbiology and Biotechnology* **88**, 977–984 (2010).

17. R.M. Tuttle, J.K. Waselenko, P. Yosseffi, N. Weigand, and R.K. Martin, "Preservation of Nucleic Acids for Polymerase Chain Reaction after Prolonged Storage at Room Temperature," *Diagnostic Molecular Pathology* **7**, 302–309 (1998).

18. P.H. Von Hippel and K.-Y. Wong, "Neutral Salts – Generality of Their Effects on Stability of Macromolecular Conformations," *Science* **145**, 577–580 (1964).

19. C.A. Whittier, W. Horne, B. Slenning, M. Loomis, and M.K. Stoskopf, "Comparison of Storage Methods for Reverse-Transcriptase PCR Amplification of Rotavirus RNA from Gorilla (*Gorilla g. gorilla*) Fecal Samples," *Journal of Virological Methods* **116**, 11–17 (2004).

20. C.J. Fregeau, H. Vanstone, S. Borys, D. McLean, J.A. Maroun, H.C. Birnboim, and R.M. Fourney, "AmpFlSTR® Profiler Plus™ and AmpFlSTR® COfiler™ Analysis of Tissues Stored in GenoFix™, a New Tissue Preservation Solution for Mass Disaster DNA Identification," *Journal of Forensic Sciences* **46**, 1180–1190 (2001).

21. V. Vincek, M. Nassiri, M. Nadji, and A.R. Morales, "A Tissue Fixative that Protects Macromolecules (DNA, RNA, and Protein) and Histomorphology in Clinical Samples," *Laboratory Investigation* **83**, 1427–1435 (2003).

22. J.H. Crowe, J.F. Carpenter, and L.M. Crowe, "The Role of Vitrification in Anhydrobiosis," *Annual Review of Physiology* **60**, 73–103 (1998).

23. T.E. Andrisin, L.M. Humma, and J.A. Johnson, "Collection of Genomic DNA by the Noninvasive Mouthwash Method for Use in Pharmacogenetic Studies," *Pharmacotherapy* **22**, 954–960 (2002).

24. D.S. Bachoon, F. Chen, and R.E. Hodson, "RNA Recovery and Detection of mRNA by RT-PCR from Preserved Prokaryotic Samples," *FEMS Microbiology Letters* **201**, 127–132 (2001).

25. S.D. Blacksell, S. Khounsy, and H.A. Westbury, "The Effect of Sample Degradation and RNA Stabilization on Classical Swine Fever Virus RT-PCR and ELISA Methods," *Journal of Virological Methods* **118**, 33–37 (2004).

26. L. Brannon-Peppas, B. Ghosn, K. Roy, and K. Cornetta, "Encapsulation of Nucleic Acids and Opportunities for Cancer Treatment," *Pharmaceutical Research* **24**, 618–627 (2007).

27. R.T. Chacko, J. Ventura, J.M. Zhuang, and S. Thayumanavan, "Polymer Nanogels: A Versatile Nanoscopic Drug Delivery Platform," *Advanced Drug Delivery Reviews* **64**, 836–851 (2012).

28. J.M. Coller, N.K. Gray, and M.P. Wickens, "mRNA Stabilization by Poly(A) Binding Protein is Independent of Poly(A) and Requires Translation," *Genes & Development* **12**, 3226–3235 (1998).

29. S.R. Florell, C.M. Coffin, J.A. Holden, J.W. Zimmermann, J.W. Gerwels, B.K. Summers, D.A. Jones, and S.A. Leachman, "Preservation of RNA for Functional Genomic Studies: A Multidisciplinary Tumor Bank Protocol," *Modern Pathology* **14**, 116–128 (2001).

30. A.E. Krafft, K.L. Russell, A.W. Hawksworth, S. McCall, M. Irvine, L.T. Daum, J.L. Connoly, A.H. Reid, J.C. Gaydos, and J.K. Taubenberger, "Evaluation of PCR Testing of Ethanol-Fixed Nasal Swab Specimens as Augmented Surveillance Strategy for Influenza Virus and Adenovirus Identification," *Journal of Clinical Microbiology* **43**, 1768–1775 (2005).

31. W.C. Ma, M. Wang, Z.Q. Wang, L.H. Sun, D. Graber, J. Matthews, R. Champlin, Q. Yi, R.Z. Orlowski, L.W. Kwak, D.M. Weber, S.K. Thomas, J. Shah, S. Komblau, and R.E. Davis, "Effect of Long-term Storage in TRIzol on Microarray-Based Gene Expression Profiling," *Cancer Epidemiology, Biomarkers & Prevention* **19**, 2445–2452 (2010).

32. J.H. Ryu, R.T. Chacko, S. Jiwpanich, S. Bickerton, R.P. Babu, and S. Thayumanavan, "Self-Cross-Linked Polymer Nanogels: A Versatile Nanoscopic Drug Delivery Platform," *Journal of the American Chemical Society* **132**, 17227–17235 (2010).

33. Y. Terui, M. Ohnuma, K. Hiraga, E. Kawashima, and T. Oshima, "Stabilization of Nucleic Acids by Unusual Polyamines Produced by an Extreme Thermophile, *Thermus thermophilus*," *Biochemical Journal* **388**, 427–433 (2005).

34. C. Tribioli and T. Lufkin, "Long-Term Room Temperature Storage of High-Quality Embryonic Stem Cell Genomic DNA Extracted with a Simple and Rapid Procedure," *Journal of Biomolecular Techniques* **17**, 249–251 (2006).

35. S.G. Wolf, D. Frenkiel, T. Arad, S.E. Finkel, R. Kolter, and A. Minsky, "DNA Protection by Stress-Induced Biocrystallization," *Nature* **400**, 83–85 (1999).

36. A.V. Kabanov and S.V. Vinogradov, "Nanogels as Pharmaceutical Carriers: Finite Networks of Infinite Capabilities," *Angewandte Chemie-International Edition* **48**, 5418–5429 (2009).

37. K. Khosravi-Darani, A. Pardakhty, H. Honarpisheh, V. Rao, and M.R. Mozafari, "The Role of High-Resolution Imaging in the Evaluation of Nanosystems for Bioactive Encapsulation and Targeted Nanotherapy," *Micron* **38**, 804–818 (2007).

38. C.S. Lengsfeld, M.C. Manning, and T.W. Randolph, "Encapsulating DNA within Biodegradable Polymeric Microparticles," *Current Pharmaceutical Biotechnology* **3**, 227–235 (2002).

39. M.L. Tan, P.F.M. Choong, and C.R. Dass, "Review: Doxorubicin Delivery Systems Based on Chitosan for Cancer Therapy," *Journal of Pharmacy and Pharmacology* **61**, 131–142 (2009).

40. L. Xu and T. Anchordoquy, "Drug Delivery Trends in Clinical Trials and Translational Medicine: Challenges and Opportunities in the Delivery of Nucleic Acid-Based Therapeutics," *Journal of Pharmaceutical Sciences* **100**, 38–52 (2011).

41. H.S. Stevenson, Y. Wang, R. Muller, and D.C. Edelman, "Long-Term Stability of Total RNA in RNAstable® as Evaluated by Expression Microarray," *Biopreservation and Biobanking* **13**, 114–122 (2015).

42. B. Roder, K. Furuhwirth, C. Vogle, M. Wagner, and P. Rossmanith, "Impact of Long-Term Storage on Stability of Standard DNA for Nucleic Acid-Based Methods," *Journal of Clinical Microbiology* **48**, 4260–4262 (2010).

43. T. Miyamoto, S. Okano, and N. Kasai, "Irreversible Thermoinactivation of Ribonuclease-A by Soft-Hydrothermal Processing," *Biotechnology Progress* **25**, 1675–1685 (2009).

44. C. Foged, H.M. Nielsen, and S. Frokjaer, "Liposomes for Phospholipase A2 Triggered siRNA Release: Preparation and In Vitro Test," *International Journal of Pharmaceutics* **331**, 160–166 (2007).

45. H. Workman and P.F. Flynn, "Stabilization of RNA Oligomers Through Reverse Micelle Encapsulation," *Journal of the American Chemical Society* **131**, 3806–3807 (2009).

46. K. Kataoka, K. Itaka, N. Nishiyama, Y. Yamasaki, M. Oishi, and Y. Nagasaki, "Smart Polymeric Micelles as Nanocarriers for Oligonucleotides and siRNA Delivery," *Nucleic Acids Symposium Series* **49**, 17–18 (Sept. 2005).

47. M. Oishi, Y. Nagasaki, K. Itaka, N. Nishiyama, and K. Kataoka, "Lactosylated Poly(ethylene glycol)-siRNA Conjugate through Acid-labile Beta-thiopropionate Linkage to Construct pH-sensitive Polyion Complex Micelles Achieving Enhanced Gene Silencing in Hepatoma Cells," *Journal of the American Chemical Society* **127**, 1624–1625 (2005).

48. T. Kasahara, T. Miyazaki, H. Nitta, A. Ono, T. Miyagishima, T. Nagao, and T. Urushidani, "Evaluation of Methods for Duration of Preservation of RNA Quality in Rat Liver Used for Transcriptome Analysis," *Journal of Toxicological Sciences* **31**, 509–519 (2006).

49. B.J. Melde, B.J. Johnson, M.A. Dinderman, and J.R. Deschamps, "Macroporous Periodic Mesoporous Organosilicas with Diethylbenzene Bridging Groups," *Microporous and Mesoporous Materials* **130**, 180–188 (2010).

50. C. Foged, H.M. Nielsen, and S. Frokjaer, "Phospholipase A2 Sensitive Liposomes for Delivery of Small Interfering RNA (siRNA)," *Journal of Liposome Research* **17**, 191–196 (2007).

51. M. Hartmann, "Ordered Mesoporous Materials for Bioadsorption and Biocatalysis," *Chemistry of Materials* **17**, 4577–4593 (2005).

52. J. Sun, H. Zhang, R. Tian, D.D. Ma, X. Bao, D.S. Su, and H. Zou, "Ultrafast Enzyme Immobilization Over Large-Pore Nanoscale Mesoporous Silica Particles," *Chemical Communications* **12**, 1322–1324 (2006).

53. I.I. Slowing, B.G. Trewyn, and V.S.Y. Lin, "Mesoporous Silica Nanoparticles for Intracellular Delivery of Membrane-Impermeable Proteins," *Journal of the American Chemical Society* **129**, 8845–8849 (2007).

54. A.B. Fuertes, P. Valle-Vigon, and M. Sevilla, "Synthesis of Colloidal Silica Nanoparticles of a Tunable Mesopore Size and their Application to the Adsorption of Biomolecules," *Journal of Colloid and Interface Science* **349**, 173–180 (2010).

55. B.G. Trewyn, I.I. Slowing, S. Giri, H.T. Chen, and V.S.Y. Lin, "Synthesis and Functionalization of a Mesoporous Silica Nanoparticle Based on the Sol-Gel Process and Applications in Controlled Release," *Accounts of Chemical Research* **40**, 846–853 (2007).

56. I.I. Slowing, B.G. Trewyn, S. Giri, and V.S.Y. Lin, "Mesoporous Silica Nanoparticles for Drug Delivery and Biosensing Applications," *Advanced Functional Materials* **17**, 1225–1236 (2007).

57. J. Rosenholm, C. Sahlgren, and M. Linden, "Cancer-Cell Targeting and Cell-Specific Delivery by Mesoporous Silica Nanoparticles," *Journal of Materials Chemistry* **20**, 2707–2713 (2010).

58. J.M. Rosenholm, C. Sahlgren, and M. Linden, "Towards Multifunctional, Targeted Drug Delivery Systems Using Mesoporous Silica Nanoparticles — Opportunities and Challenges," *Nanoscale* **2**, 1870–1883 (2010).

59. F. Gao, P. Botella, A. Corma, J. Blesa, and L. Dong, "Monodispersed Mesoporous Silica Nanoparticles with Very Large Pores for Enhanced Adsorption and Release of DNA," *Journal of Physical Chemistry B* **113**, 1796–1804 (2009).

60. C.E. Ashley, E.C. Carnes, K.E. Epler, D.P. Padilla, G.K. Phillips, R.E. Castillo, D.C. Wilkinson, B.S. Wilkinson, C.A. Burgard, R.M. Kalinich, J.L. Townson, B. Chackerian, C.L. Willman, D.S. Peabody, W. Wharton, and C.J. Brinker, "Delivery of Small Interfering RNA by Peptide-Targeted Mesoporous Silica Nanoparticle-Supported Lipid Bilayers," *ACS Nano* **6**, 2174–2188 (2012).

61. Z. Li, J.C. Barnes, A. Bosoy, J.F. Stoddart, and J.I. Zink, "Mesoporous Silica Nanoparticles in Biomedical Applications," *Chemical Society Reviews* **41**, 2590–2605 (2012).

62. C.T. Kresge, M.E. Leonowicz, W.J. Roth, J.C. Vartuli, and J.S. Beck, "Ordered Mesoporous Molecular Sieves Synthesized by a Liquid-Crystal Template Mechanism," *Nature* **359**, 710–712 (1992).

63. M.C. Burleigh, M.A. Markowitz, E.M. Wong, J.S. Lin, and B.P. Gaber, "Synthesis of Periodic Mesoporous Organosilicas with Block Copolymer Templates," *Chemistry of Materials* **13**, 4411–4412 (2001).

64. Y. Goto and S. Inagaki, "Synthesis of Large-Pore Phenylene-Bridged Mesoporous Organosilica Using Triblock Copolymer Surfactant," *Chemical Communications* **20**, 2410–2411 (2002).

65. Q.S. Huo, D.I. Margolese, and G.D. Stucky, "Surfactant Control of Phases in the Synthesis of Mesoporous Silica-Based Materials," *Chemistry of Materials* **8**, 1147–1160 (1996).

66. B.J. Johnson, B.J. Melde, M.A. Dinderman, and B. Lin, "Stabilization of RNA through Absorption by Functionalized Mesoporous Silicate Nanospheres," *PLoS One* **7**, e50356, (2012).

67. K. Nakanishi, Y. Kobayashi, T. Amatani, K. Hirao, and T. Kodaira, "Spontaneous Formation of Hierarchical Macro-Mesoporous Ethane-Silica Monolith," *Chemistry of Materials* **16**, 3652–3658 (2004).

68. B.J. Johnson, B.J. Melde, P.T. Charles, M.A. Dinderman, A.P. Malanoski, I.A. Leska, and S.A. Qadri, "Macroporous Silica for Concentration of Nitroenergetic Targets," *Talanta* **81**, 1454–1460 (2010).

69. B.J. Johnson, B.J. Melde, G.W. Peterson, B.J. Schindler, and P. Jones, "Functionalized Organosilicate Materials for Irritant Gas Removal," *Chemical Engineering Science* **68**, 376–382 (2012).

70. T. Amatani, K. Nakanishi, K. Hirao, and T. Kodaira, "Monolithic Periodic Mesoporous Silica with Well-Defined Macropores," *Chemistry of Materials* **17**, 2114–2119 (2005).

71. K. Nakanishi, T. Amatani, S. Yano, and T. Kodaira, "Multiscale Templating of Siloxane Gels via Polymerization-Induced Phase Separation," *Chemistry of Materials* **20**, 1108–1115 (2008).

72. B.J. Johnson, I.A. Leska, B.J. Melde, R.L. Siefert, A.P. Malanoski, M.H. Moore, J.R. Taft, and J.R. Deschamps, "Extraction of Perchlorate Using Porous Organosilicate Materials," *Materials* **6**, 1403–1419 (2013).

73. M.C. Burleigh, S. Dai, E.W. Hagaman, and J.S. Lin, "Imprinted Polysilsesquioxanes for the Enhanced Recognition of Metal Ions," *Chemistry of Materials* **13**, 2537–2546 (2001).

74. H.G. Zhu, D.J. Jones, J. Zajac, R. Dutartre, M. Rhomari, and J. Roziere, "Synthesis of Periodic Large Mesoporous Organosilicas and Functionalization by Incorporation of Ligands into the Framework Wall," *Chemistry of Materials* **14**, 4886–4894 (2002).

75. B.J. White, B.J. Melde, M.H. Moore, and G.W. Peterson, "Functionalized Organosilicate Sorbents for Air Purification," NRL/FR/6920--13-10,251, U.S. Naval Research Laboratory, Washington, DC, Dec. 23, 2013.

76. J. Kobler, K. Möller, and T. Bein, "Colloidal Suspensions of Functionalized Mesoporous Silica Nanoparticles," *ACS Nano* **2**, 791–799 (2008).

77. H. Venner and C. Zimmer, "Studies on Nucleic Acids .8. Changes in Stability of DNA Secondary Structure by Interaction with Divalent Metal Ions," *Biopolymers* **4**(3), 321–335 (1966).

78. B. Lin, B.J. Johnson, B.J. Melde, G.M. Haas, M.K.J. McConner, and J.R. Taft, "Adsorption and Elution of Nucleic Acids: Mesoporous Materials and Methods," *Open Access Journal of Science and Technology*, in press, 2016.

79. X. Tang, S.L. Morris, J.J. Langone, and L.E. Bockstahler, "Simple and Effective Method for Generating Single-Stranded DNA Targets and Probes," *BioTechniques* **40**, 759–763 (2006).

80. H.J. Kim and G. Guiochon, "Comparison of the Thermodynamic Properties of Particulate and Monolithic Columns of Molecularly Imprinted Copolymers," *Analytical Chemistry* **77**, 93–102 (2005).

81. R.J. Umpleby, S.C. Baxter, M. Bode, J.K. Berch, R.N. Shah, and K.D. Shimizu, "Application of the Freundlich Adsorption Isotherm in the Characterization of Molecularly Imprinted Polymers," *Analytica Chimica Acta* **435**, 35–42 (2001).

82. M.C. Moran, M.G. Miguel, and B. Lindman, "Surfactant-DNA Gel Particles: Formation and Release Characteristics," *Biomacromolecules* **8**, 3886–3892 (2007).

83. X. Li, J. Zhang, and H. Gu, "Study on the Adsorption Mechanism of DNA with Mesoporous Silica Nanoparticles in Aqueous Solution," *Langmuir* **28**, 2827–2834 (2012).

84. A. Masotti, F. Bordi, G. Ortaggi, F. Marino, and C. Palocci, "A Novel Method to Obtain Chitosan/DNA Nanospheres and a Study of Their Release Properties," *Nanotechnology* **19** (2008).

85. S. Wu, X. Huang, and X. Du, "Glucose- and pH-Responsive Controlled Release of Cargo from Protein-Gated Carbohydrate-Functionalized Mesoporous Silica Nanocontainers," *Angewandte Chemie-International Edition* **52**, 5580–5584 (2013).

86. F. Pu, Z. Liu, J. Ren, and X. Qu, "Nucleic Acid-Mesoporous Silica Nanoparticle Conjugates for Keypad Lock Security Operation," *Chemical Communications* **49**, 2305–2307 (2013).

87. A.d.A. Correa and M.P. Miagostovich, "Optimization of an Adsorption-Elution Method with a Negatively Charged Membrane to Recover Norovirus from Lettuce," *Food and Environmental Virology* **5**, 144–149 (2013).

88. J. Sambrook, E.F. Fritsch, and T. Maniatis, *Molecular Cloning: A Laboratory Manual*, 2nd ed., 3 vols. (Cold Spring Harbor Laboratory Press, Cold Spring Harbor, New York, 1989).